AD-A131 739 RESEARCH AND DEVELOPMENT FOR INVESTIGATIONS OF METALLIC 1/1
ADSORPTIONS ON ME..(U) PARIS-6 UNIV (FRANCE)
LABORATOIRE D'OPTIQUE DES SOLIDES F ABELES ET AL.
UNCLASSIFIED JUN 83 DAJA37-79-C-0516 F/G 7/4 NL

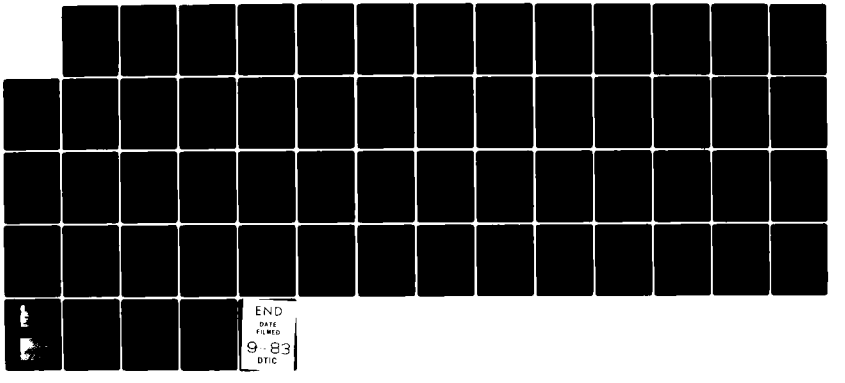

END
DATE FILMED
9-83
DTIC

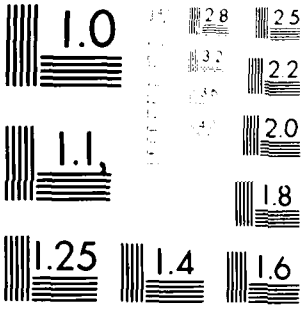

RESEARCH AND DEVELOPMENT FOR INVESTIGATIONS OF METALLIC ADSORPTIONS ON METAL SURFACES BY OPTICAL TECHNIQUES COMPLEMENTED BY d.c. RESISTIVITY AND AUGER SPECTROSCOPY.

Final Technical Report

by

F. ABELES
T. LOPEZ-RIOS
Y. BORENSZTEIN
G. VUYE

June 1983

EUROPEAN RESEARCH OFFICE
United States Army
London, England

Contract n° DAJA37-79-C-0516

Laboratoire d'Optique des Solides, Université P. et M. Curie
Paris, France

Approved for Public Release; distribution unlimited

REPORT DOCUMENTATION PAGE

READ INSTRUCTIONS BEFORE COMPLETING FORM

1. REPORT NUMBER	2. GOVT ACCESSION NO. AD-A131 139 / 3. RECIPIENT'S CATALOG NUMBER
4. TITLE (and Subtitle) Research & Development for Investigations of Metallic Adsorptions on Metal Surfaces by Optical Techniques Complemented by d.c. Resistivity and Auger Spectroscopy	5. TYPE OF REPORT & PERIOD COVERED Final Report, June 1983 / 6. PERFORMING ORG. REPORT NUMBER
7. AUTHOR(s) F. Abeles, T. Lopez-Rios, Y. Borensztein, G. Vuye	8. CONTRACT OR GRANT NUMBER(s) DAJA37-79-C-0516
9. PERFORMING ORGANIZATION NAME AND ADDRESS Laboratoire d'Optique des Solides, U. P. et M. Curie, Paris, France	10. PROGRAM ELEMENT, PROJECT, TASK AREA & WORK UNIT NUMBERS 1T161102BH57-05
11. CONTROLLING OFFICE NAME AND ADDRESS USARDSG-UK Box 65, FPO NY 09510	12. REPORT DATE June 1983 / 13. NUMBER OF PAGES Fifty-Four (54)
14. MONITORING AGENCY NAME & ADDRESS(if different from Controlling Office)	15. SECURITY CLASS. (of this report) UNCLASSIFIED / 15a. DECLASSIFICATION DOWNGRADING SCHEDULE

16. DISTRIBUTION STATEMENT (of this Report)

Approved for Public Release; Distribution Unlimited

17. DISTRIBUTION STATEMENT (of the abstract entered in Block 20, if different from Report)

18. SUPPLEMENTARY NOTES

19. KEY WORDS (Continue on reverse side if necessary and identify by block number)

20. ABSTRACT (Continue on reverse side if necessary and identify by block number)

Differential reflectivity $\Delta R/R$ measurements between a smooth Ag surface and the same surface covered by silver deposits of various thicknesses were performed in ultra high vacuum over the 1.5-5 eV spectral range for different Ag substrate temperatures in order to examine roughness effects on the electromagnetic field.

Abstract

Differential reflectivity Δ R/R measurements between a smooth Ag surface and the same surface covered by silver deposits of various thicknesses were performed in ultra high vacuum over the 1.5 - 5 eV spectral range for different Ag substrate temperatures.

One silver monolayer on silver substrate at 125 K gives rise to relatively large changes in reflectivity ($\sim 10^{-3}$).
For thicker deposits (from 4 monolayers up) a well defined absorption at 3.5 eV due to surface plasmon excitation is found. The experimental results are compared to computed values of Δ R/R. Some structures found in the vicinity of the Ag surface plasmon frequency are interpreted as a surface plasmon splitting due to the surface roughness.

Δ R/R variations during samples annealing to room temperature are also investigated and compared to the reported d.c resistance and SERS measurements. Roughness was also investigated by electron microscopy by "pinning" the surface at T = 140K with a superficial oxyde. An additional absorption found for thick ($\sim 10^3$ Å) quenched silver films is attributed to a surface effect.

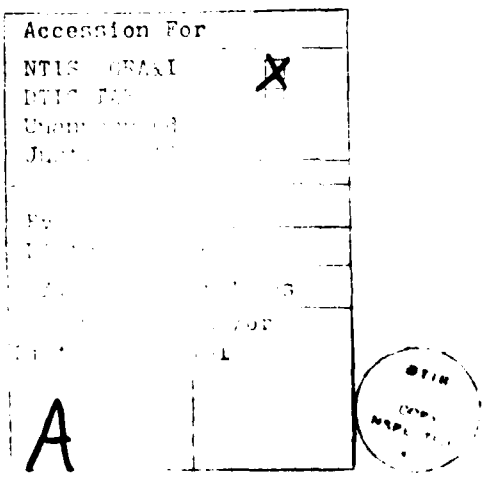

I - INTRODUCTION

A large amount of work has been already performed in order to understand the optical properties of a flat surface. This problem is particulary complicate for p-polarized light and a careful analysis requires a non-local formalism describing the surface region via a dielectric function depending on frequency and wave vector. Nevertheless in most practical cases the classical Fresnel formulas are a good description of the reflection of light on a good metallic mirror. In fact a flat surface is an abstraction and all real surfaces have some roughness, on the light wave-length scale, and this is the real incentive to the study of roughness effects on surface phenomena, like electronic or vibrational properties of molecules on a rough surface.

For instance, when investigating the electronic properties of adsorbates by reflectivity measurements one relates the observed absorptions to electronic transitions between electronic states of the adsorbate and/or the surface. The optical absorption of a molecule is given by $\mathrm{Im}\,(\alpha)\,E^2$, where α is the molecule polarizability and E the field seen by the molecule. For a flat surface E can be known from the Fresnel formulas and it is usually slowly varying with frequency. This is not the case for a rough surface where optical absorption depends, besides the values of $\mathrm{Im}\,(\alpha)$ on the values of E at the molecule site, the resulting effect depending on the average of the local fields for all adsorption sites. The local field E is in general a complicated function depending on the surface shape. It can reach very high values, for instance in the neighbourghood of a needle like in lightning-rod effect.

There are a large number of theorical methods to investigate the electromagnetic properties of rough surfaces and much of experimental work has already been devoted to the caracterization of different kinds of roughness using light waves. Very often these

studies are related to surface polaritons excitation or interaction with roughness. A recent theoretical review can be found in the paper by Maradudin(1) and experimental aspects are discussed by Raether (2). A simple theory very often used is the "Scalar scattering theory ". This considers only the phase modulation of the incident and outgoing light by interface shape. In the frame of the scalar theory, the scattered light and the specular beam are independant of light polarization depending on the roughness height only. This theory is a long wave limit theory and does not take into account the possible excitation of surface modes which are the main effect found in the experiments discussed in this paper. In contradistinction, rigourous theories based on the extinction theorem, require a large amount of computational work even for periodic gratings leading to numerical results which are not always very accurate.In order to interpret the results to be presented here, we have made use of a perturbative theory due to Kröger and Kretschmann (3).

In the past most investigations were devoted to electromagnetic fields far from the surface, but in order to understand the optical properties of adsorbates some authors have studied the near field on reflecting rough surfaces. The near field for silver grating surfaces of different shapes was already computed (4,5).

An other approach of a rough surface is to consider a protuberance on a flat surface. Berreman (6,7) considered a hemispherical bump on otherwise smooth surfaces for several dielectric material in the electrostatic approximation. He found resonant frequencies related to the bump modes. Ruppin (8) computed, again in the electrostatic approximation, the electromagnetic field at the surface of a hemispherical bump on a flat surface for Ag, Au, Na and found fields enhancement strongly depending on the light frequency. Gersten and Nitzan (9) studied, also neglecting retardation, the case of an hemiellipsoid on a perfectly conducting plane and found very high values of the extinction coefficient and of the electric field at the surface depending on the hemiellipsoidal

shape. Kerker et al (10), using electromagnetic theory, studied the scattering of plane wave by a Ag sphere and found again a resonant behaviour as a function of frequency. With minor modifications, Kerker et al (10) results can be applied to a hemisphere on a perfectly conducting medium. Obviously, in the general case, a rough surface cannot be considered as being made of isolated protuberances, because each irregularity receives the fields which are scattered from the neighbouring bumps. This should be particularly true at the resonance frequency of the bumps. Nevertheless it is clear that a rough surface can support localized electromagnetic resonances (surface polaritons resonances localized at the surface irregularities) in a manner similar to the well known resonances on colloidal particles (11). This point was probably first demonstrated experimentally in the work of Beaglehole and Hunderi on light scattering by rough surfaces (12,13). Recently we were able to estimate the field enhancement at the quenched silver film surface by measuring the reflectivity changes induced by Cu adsorbates for 0.1-1 monolayer coverage (14).

An other effect related to rough surfaces is the possible excitation of surface plasmon waves. These propagating surface modes exist at the flat surface of a free electron metal, but cannot be excited by light. For a rough surface this posibility exists as first pointed out by Fano (15) in order to explain the Wood anomalies of gratings. For a wave impinging a flat surface at an angle θ the wave vector k parallel to the surface is in all cases equal to $\omega/c \sin\theta$ whereas on a rough surface there are, beside the diffrated orders, with wave vector $k<\omega/c$ leading to the scattered light, other wave with $k<\omega/c$ which are evanescent in the direction normal to the surface and with a wave vector parallel to the surface large enough to excite surface plasmon waves. It must be underlined that this kind of excitations are propagating modes travelling along the surface in contradistinction to the already mentioned localized modes at the bumps.

Another interesting phenomenon occurring at rough surfaces only and not yet well understood is the surface enhanced Raman scattering

(SERS) effect. It is clear now that a rough surface is a prerequisite to the occurence of SERS, but not all rough surfaces give rise to SERS and a point still under discussion is what kind of roughness is involved in SERS. An overview of the actual situation in SERS investigations can be found in a recent paper by Otto (16). SERS was first observed on Ag surfaces roughened by an electrochemical treatment (17), then it was reported on silver deposited on CaF_2 (18) and in some cases on mechanically polished Ag (19). Another method to obtain surfaces with very high ($\sim 10^6$) Raman cross-section enhancement is by quenching Ag on substrates cooled in liquid nitrogen temperatures (20). An optical study of this kind of surface has already been briefly reported (21), and will be developped in details in this paper. In particular we are interested in the roughening of silver surfaces by quenching at about 140K small Ag deposits (few monolayers).At this temperature, many faults are created during the crystal growth producing some roughness on the atomic scale, the roughness becoming macroscopic for thicker deposits. To study very small roughness producing very small modifications of reflectivity($\sim 10^{-4}$), we employed a differential technic Differential reflectivity measurements were first employed to investigate the electronic properties of diluted alloys (22,23) and also for surface roughness studies (12). The avantages of differential measurements of reflectivity were used by several groups (24,25,26) to investigate gas adsorption on surfaces kept under ultra-high vacuum.

In section II we describe the experimental set-up : the ultra-high vacuum system and the differential reflectometer. Section III is devoted to a discussion of roughening induced by thin silver deposits,the annealing of these deposits being examined in section IV. Section V contains a comparison between experimental results and numerical calculations performed with the Kröger and Kretschmann formalism. Finally we investigate in section VI the topography of quenched silver surfaces and their relationship with the observed optical absorptions.

II EXPERIMENTAL

a) The ultra high vacuum chamber

Our samples are prepared and studied in a stainless steel ultra high vacuum system working at pressures in the low 10^{-10} torr range. Pumping is assured by a 200l/sec ion pump, a titanium sublimation pump and liquid nitrogen cryotraps. A four-grid LEED-Auger spectrometer with a grazing incidence electron gun is currently used for Auger surfaces analysis. Details of this equipment can be found in ref (27). A high precision goniometer ($\sim 4\ 10^{-2}$ degrees) allows to perform optical measurements as a function of the angle of incidence, for different polarizations of light, as described in ref (27), but the results which will be presented in this paper were performed at normal incidence only . Another facility of this equipment is to allow Raman studies with a spectrograph especially attached to the vacuum chamber.

b) Samples preparations

The Ag surfaces and superficial layers of Ag , Al and Cu have been prepared evaporating these metals on glass or fused silica substrates with two crucibles located at a distance of approximately 33 cm from the substrates. Carefully polished glass or fused silica plates are placed on a copper holder cooled by a copper plate in contact with a small liquid nitrogen reservoir. To ensure a better thermal contact several indium tips are inserted between the Cu holder and the silica substrate. The temperature is measured at the glass/vacuum interface by a Cu-constantan thermocouple. Temperatures as low as 120 K are generally obtained. When stopping the pumping on the capilar ensuring the filling of the liquid nitrogen recipient, room temperature is reached in about 3 hours. Glass or silica substrates are

cleaned with a method currently employed in the laboratory. It consists in rubbing the surface with a mixture of sodium hydroxyde and calcium carbonate, then rincing with $H NO_3$ and finally with desionized water. The crucibles are shielded by cold liquid nitrogen walls. The pressure during metal deposition is lower than 10^{-9} torr. The monitoring of the thickness of the metal deposits is performed with a 5 MHz sloan oscillating quartz located at about 21 cm from the crucibles in order to increase the sensibility of the thickness measurements. A shutter allows to evaporate on the whole surface of the sample or just on one half as needed for differential reflectivity measurements which will be discussed later. Depending on the position of this shutter it is possible to evaporate at the same time on the sample and/or on a spare glass plate. The thickness of the metal film on the spare glass is determined with approximately 1% accuracy by X-ray interference in reflection at grazing incidence (Kiessig method (28)). These measurements allow the accurate calibration of the quartz microbalance. Typical values of this calibration are 14 Hz/ Å for Ag, 12 Hz/Å for Cu and 3,7 Hz/Å for Al. In the present experiments we did not perform the quartz microbalance calibration for each experiment, therefore the indicated thickness are estimated to 5 %. The surfaces under investigation are those of Ag films about 0.1 µm thick evaporated on substrates kept at room temperature. The silver films are made of many microcrystals with lateral dimensions about 0.5 µm with the axis [111] nearly perpendicular to the substrate surface but randomly oriented on the substrate planes. Therefore our surfaces will behave essentially as (1,1,1) single crystals surfaces. Microstereographic studies of carbon replicas of samples similar to ours (29) indicated that roughness is definitely smaller than 30 Å, the main irregularities occurring at the grains boundaries. The investigation of the roughning of these rather smooth surfaces by quenching at T = 140 K various amounts of silver is one of the aims of the work described in this paper.

C- Optical set-up

The principle of the set-up used for differential reflectivity experiments is represented on fig.1. A monochromatic beam is focused on a mirror vibrating at 800 Hz (manufactured by General Scanning, model G 112) which sends the beam up and down on the reflecting sample. The beam is alternatively reflected on two halves of a sample (A and B) having a small difference on reflectivity ($R_A \neq R_B$) before being focused on a photomultiplier (PM). The vibrating mirror and the photomultiplier being optically conjugated, the beams reflected by the A and B areas of the sample impinge on the same point of the photomultiplier and this is a necessary condition in order to avoid spurious signals. A feed back on the high voltage of the photomultiplier maintains a constant mean value of the delivered current as usual in modulation spectroscopy. A lock-in amplifier detection at the frequency of the vibrating mirror, combined with the mentioned feed back on the PM high voltage supply gives a signal proportional to $\Delta R/R = 2(R_A-R_B)/(R_A+R_B)$. In order to have absolute values of $\Delta R/R$, we need a calibration operation. This is performed with a spectrophotometer included in the apparatus and allowing to measure absolute values of the reflectivity. We will return to this point later. The insert indicates the shape of the photomultiplier output. The details of the optical mounting are represented in figure 2. The sample is located at the center of the U.H.V system and the same window is used for the entrance into and the exit of the light. We have used a Xe lamp (Osram X BO75) in the 0.28 - 0.4 µm spectral range (S_1) and a W-ribbon source (Osram 250 W) (S_2) in the 0.4-0.9 µm région. The monochromator is a Coderg (f = 0.3 m) of aperture f/5 equipped with a holographic grating (1800 lines/mm) with great efficiency at 250 nm and a grooved grating (1800 lines/mm) blazed at 550 nm. The mirrors m_1 and m_2 provide an image 0' of the monochromator slit 0 on the vibrating mirror M. The vertical dimension of the ouput slit was limited to approximately 0.5 mm and the image 0' on the vibrating mirror M is about 2x2 mm. The mirrors m_4 and m_5 focuse the oscillating

beam, after reflection on the sample, on the P.M (EMI 9659QB). A ground fused silica plate is located in front of the PM photocathode in order to minimize any spurious effects due to the vibrating beam.

A beam-splitter M' can be inserted in the path of the optical beam to collect part of the incident light and to allow measuring with a double beam technique the absolute value of the reflectivity. The chopper C modulates at different frequencies the two beams before reaching the photomultiplier and lock-in amplifier detections with feed-back preamplifier control allow to obtain the intensity ratio of the beams (see ref. 27). Calibrations of differential spectra are obtained with mirror M at rest by measuring the reflectivity on areas A and B of the sample (position up and down) when the reflectivity difference between them is high enough to have a good accuracy (typically 10 to 20 %). We should like to point out this method which allows calibration of differential spectra, generally a difficult task with a reasonably good accuracy (∿ 2 %).

III - THIN SILVER DEPOSITS ON SILVER

In a first series of experiments, we have prepared thin films about 0.1 μm thick by condensing silver onto well polished fused silica substrates kept at room temperature. The structure of these films was discussed in chapter II. We will indicate later that in the neighbourhood of the plasma frequency films even as thick as 0.1 μm cannot be considered, from the optical point of view, as semiinfinite media, but this fact is irrelevant for the problems investigated on this paper. We did not prepare thicker films in order to avoid transmitted light at the plasma frequency because we were interested in starting with a surface as flat as possible and generally roughness increases with film thickness (30). In order to investigate the early stages of roughening of a Ag surface we have prepared simultaneously at room temperature two Ag surfaces which were afterwards cooled to about 140K. At this temperature we have quenched on half of the

surface various amounts of silver in order to carry out differential reflectivity measurements. Fig 3 shows $\Delta R/R$ vs $\hbar\omega$ measured with a Ag substrate 836 Å thick at T = 125 K for deposits of 2.6, 10.8 and 19 Å of silver (one monolayer = 2.35 Å) quenched at a rate of 0.7 Å/sec. To understand the real significance of these curves one should keep in mind that $\Delta R/R$ gives also the structures of R and remember that reflectivity of bulk Ag reaches very small values in the vinicity of the plasmafrequency ($\hbar\omega$ = 3.79 eV) leading to greatly enhanced values of $\Delta R/R$ even for very small ΔR. The insert in fig 3 shows the bulk silver reflectance R vs $\hbar\omega$. The two sharp peaks with opposite signs in $\Delta R/R$ (for 10.8 Å and 19 Å they are out of the drawing) are mainly due to :

i) the finite thickness of the silver substrate,

i.i) the slight difference in optical constants between the quenched films and bulk silver,

i.i.i) roughness induced by the silver deposits.

The main contribution to the $\Delta R/R$ structure around 3.9 ev arises from the first two contributions. The two peaks do not describe any surface effect and are of no interest to the subject investigated in this paper, nevertheless we will discuss this point again in chapter V with the help of some numerical calculations. In fig. 3 we notice that an optical absorption due to the surface deposit itself starts at $\hbar\omega$ = 3.6 eV for the two thicker layers (10.8 Å and 19 Å) absorption is clearly due to surface plasmon excitation by roughness, a point well documented today (31). In chapter V we will clearly show that the minimum is not influenced by the finite thickness of the substrate and is nearly independent of the optical constants.

It was indicated above that our surfaces have mainly a cristallographic (1,1,1) structure. Beside faults mainly located at grain - boundaries, each single crystal (about 0.1 µm diameter) has large terraces separated by atomic steps with a large number kink sites. When a foreign atom is adsorbed on a terrace it has a probability ν_1 to migrate to an other site given by $\nu_1 = \nu_0 \exp(-E/kT)$ where

E is an activation energy, k and T [illegible] the Boltzmann constant and temperature respectively. Different resistivity measurement (32) have shown that Au isolated adatoms on gold(1,1,1) vicinal surfaces migrate at temperatures $T \gtrsim 20K$. We can expect similar values of the activation energy for silver [illegible] and we conclude that we do not have isolated adatoms on our surface. Nevertheless the growth of a superficial layer is a dynamic phenomenon with two competing processes namely the atoms condensation on an adatom position given by the evaporation rate $f = \frac{dn}{dt}$ and adatoms migration to a kink site position governed by the jump probability ν_1 exponentially dependant of temperature. Chauvineau (33) has recently performed a computer simulation of crystal growth on vicinal surfaces with a model with random migration and condensation depending on the ratio $K = \nu_1/f$ only and he found for high mobility (high K) monolayer by monolayer growth and atomic roughness oscillating periodically with the deposited thickness with a monolayer period (flat for a full monolayer, rough for one half of a monolayer). For low mobility an increase of the macroscopic roughness with thickness was found. For a very low mobility ($\nu_1 = 0$), we can expect that the root mean square of the roughness height increases as the square root of the deposit thickness. Fig. 3 shows that even for a monolayer coverage the induced roughness induces important optical effects. For this coverage surface plasmons are apparently not efficiently excited. We estimate that at this low coverage the observed effect is related to the surface electronic structure induced by atomic faults like atoms with broken bonds. This is an interesting point which should be investigated at liquid He temperature at which one has for low coverages a large number of isolated adatoms on the terraces.

To illustrate the influence of the mobility on roughness growth we have performed the same kind of experiments at room temperature and the results are indicated in fig.4. At 3.9 eVand 4.1eV We have again the two peaks which are irrelevant for the questions discussed here, but we have also an optical absorption starting at 3.7 eV with a maximum at 3.6 eV, and clearly related to surface plasmon excitation. We have thoroughly investigated whether this structure originates from unexpected reasons like roughness of the starting surface combined with size effects and we have concluded that the minimum at 3.6 eV is, indeed,

induced by an increase of resistance due to the Ag deposit. A first point to underline here is that this effect is very much smaller than at T = 140K as can be seen on comparing, in fig. 3 and 4 the thicknesses and intensities of the 3.6 eV peak. For Ag coverages in the monolayer range, we should do not any effect at T = 300 K whereas a quite sizeable signal is obtained at T = 140 K.

It is known that the d.c resistance of thin films (a few hundred Å thick) depends not only on the metal resistivity but also on the more or less specular reflection of the conduction electrons on the surface that is to say on the atomic roughness seen by the free electrons (34).

If the absorbed atoms on a thin film surface induce a less specular reflection of the conduction electrons, the d.c resistance can increase even if the mean thin film thickness increases also. Resistance measurements at 300 K during Au deposition in U.H.V on Au thin films (35) and of Ag on Ag thin films (36) gives a decrease of the resistance with increasing thickness, the result being assigned to the increase of thickness only. From the present experiments it appears that some roughness occurs, which is measurable for large enough thicknesses. For high mobility and for and ideal crystal, crystal growth can take place, in principle, without faults, but, in our case, on the one hand we do not have an ideal crystal but rather a polycrystal with many faults and, on the other hand, a possible contamination of the surface, even with a very low coverage, can disturb the growth mechanism. Another important point to be underlined is that the optical absorption due to surface plasmon excitation is located over a narrow spectral region, probably indicating a roughness with relatively small scale, i.e with great wave number Fourier components. This is a surprising result that we do not well understand, because one would rather expect a large scale roughness when silver is deposited at room temperature. Fig. 5 shows experiments analogous to those of fig. 3 but

for thicker films. With increasing thickness, the minimum at 3.6 eV broadens and simultaneoustly another absorption at lower energy become more and more important eventually becoming the most important for the thickest deposit (d ≈2000 Å). This is the anomalous absorption first found by Hunderi and Myers (37) on quenched silver films and assigned by Hunderi to bulk defects. Nowadays there is a renewed interest concerning the physical origin of this optical absorption, because it is present for silver films displaying SERS and disappears on warming up the sample in the same way as SERS. Moskovits et al (38) claimed that this anomalous absorption is due to surface irregularities; anomalous absorption and surface enhanced Raman effect being two aspects of the same problem. We have shown (39) and we will discuss in section VI that anomalous absorption of quenched silver films is, indeed, a surface effect.

On the flank of the high-energy negative peak (corresponding to small values of silver reflectivity) a shoulder can be observed in fig. 5 at about 3.7 eV. It corresponds to a roughness induced a splitting of surface plasmon excitation as pointed out by Kretschmann et al (40). For a smooth surface one has a single surface electromagnetic mode, but for a rough surface, like a grating , a gap can appear in the surface dispersion curves (41). The reason of this splitting is that the incoming light can excite two surface plasmons with the same energy but with wave vectors of different directions; for instance, for a one dimensional grating two surface plasmons with opposite wave vectors. For a statistical roughness a similar effect can occur as investigated by Kretschmann et al. (40) and Maradudin et al. (42). Experimental evidence for this splitting was provided by Kōts et al. (43) for electrochemical roughening of a (1,1,1) silver electrode by anodic dissolution and subsequent redeposition of silver with a standard method employed to obtain SERS active surfaces. Roughness induced surface plasmon splitting on a K

surface was observed by Williams et al. (44) in plasma radiation excited by fast electrons (1.5 KV). In fig. 6 we examine more closely the structures in the vicinity of the Ag plasma frequency, reproducing part of fig.5(on an expanded scale in order to see better the details). In the present case, R is rapidly decreasing with increasing ω and as we have measured $\Delta R/R$, the possible absorption (minimum in ΔR) appears just as a shoulder on the $\Delta R/R$ curves. It was predicted that for a free electrons metal the two peaks are quasi symmetrically situated around the surface plasmon frequency for a flat surface ($\varepsilon = -1$). This is not the case here due to the d-band contribution to the dielectric constant of silver. The two possible plasmon absorptions are tentatively indicated by arrows. The splitting is slightly increasing with the thickness of the deposited silver overlayer from 0.15 eV for d = 19 Å to about 0.22 eV for d = 187 Å. The spectral position of the shoulder is difficult to ascertain because it is situated on a sharply decreasing curve.

Let us, now, recall some theoritical aspects of the problem at hand, taken from the work of Kretschmann et al. (40). For a flat interface between a metal with dielectric constant $\varepsilon(\omega)$ and vacuum, one has a single surface plasmon mode with a dispersion relation given by

$$\omega/c.\ n_s(\omega,k) = \varepsilon k_2 + k_1 = 0 \qquad (1)$$

where $k_1 = \left[\varepsilon \left(\frac{\omega}{c}\right)^2 - k^2\right]^{1/2}$, $k_2 = \left[\left(\frac{\omega}{c}\right)^2 - k^2\right]^{1/2}$

and k is the surface plasmon wave vector parallel to the surface. For a rough surface, the surface plasmon dispersion is no more given by eq. (1) but by :

$$n_r(\omega,k) = n_s(\omega,k) - (\varepsilon-1)^2 \langle s^2 \rangle I(k) \qquad (2)$$

where $n_s(\omega,k)$ is given by éq. (1), $\langle s^2 \rangle$ is the mean-square roughness height and I (k) is an integral over all first order scattering processes with final wave-vector k. For large wave-vectors ($k > 2\omega/c$) some simplifications can be performed on the integral I (k) and the dispersion relation for a flat surface can be approximated

by $\frac{\omega}{c} \quad n_s(k) = k(\varepsilon + 1)$ leading to :

$$\frac{\omega}{c} \cdot \frac{n_r}{k} = (\varepsilon + 1) - \left(\frac{\varepsilon - 1}{\varepsilon + 1}\right)^2 a^2 \qquad (3)$$

with $a^2 = \langle s^2 \rangle I_1 \quad (k)$

$$I_1(k) = c^2/\omega^2 \int_{k' > 2\frac{\omega}{c}} d^2 k' \; g\left(|\vec{k} - \vec{k'}|\right) kk' \quad (1 - \cos\phi)^2$$

where g is the surface-roughness correlation function and $I_1(k)$ describes all possible first order scattering processes with wave vector $k' > 2\frac{\omega}{c}$ into surface plasmons with wave vector k. ϕ is the angle between $\vec{k}$ and $\vec{k'}$. For a given value of a, the dispersion relation given eq. 3 can be verified for two values of the dielectric constant $\varepsilon_{\pm} = (1 \mp a) / (1 \pm a)$ indicating a surface plasmon splitting. Rahman and Maradudin(42) have found similar results with an equivalent surface layer model.

To obtain more information about our experimental results, we have computed, using eq. 3, the response function $c^2/\omega^2 \; |k/n_r|^2$ for different values of a and using the bulk silver dielectric constants (45). The results are shown in fig. 7. The curve corresponding to a smooth surface ($a^2 = 0$) is represented by the discontinuous line and the values of the real part of the dielectric constant is indicated on the upper scal . We see that the high frequency peak shifts slowly in energy with increasing values of a like in our experiments ; even if, as already pointed out, it is difficult to find their spectral position, they seem to have the same behaviour. The lower energy peak shifts, in our experiments, in the same way as expected from the theory. The experiments of Kötz et al. (43) were performed at a metal electrolyte interface and their surface plasmons are shifted to lower energies farther from the silver volume plasmon and from the Ag absorption edge, where surface plasmon absorption can be easier observed. From the present experiments, we found a^2 values comprised between 0.05 and 0.1, whereas Kötz et al. found $a^2 = 0.01$.

IV - ANNEALING

Interesting informations about quenched films can be obtained from the study of $\Delta R/R$ during annealing. In particular, it is possible to establish relationships with other physical parameters like d.c resistivity, light scattering or SERS intensity modifications on quenched films reported in the literature.

The annealing of quenched films, which, as we already saw, do not have a well defined crystallographic structure, is a complicated process. To be more specific, it is not possible to find an activation energy characteristic of film defects like, for instance, for vacancies on quenched silver wires (46), because we have an ensemble of heterogeneous faults. In any case, the most important defects in our films are the grain boundaries and annealing induces a growth of the larger single crystals at the expense of the smaller ones by a lateral displacement of grain boundaries, leading to a better crystallographic structure. Simultaneously, with increasing temperature surface atoms increase their surface mobility and move along the surface "from the mountain to the valley" leading to a decrease of the macroscopic roughness. We must keep in mind that, in principle, bulk annealing and surface annealing occur together leading to a supplementary difficulty in the interpretation of optical data. Foreign atoms can strongly reduce surface mobility and prevent the flattering of surface with annealing. We will employ this particularity in the experiments reported in section VI. Moreover, superficial layers can "pin" bulk defects ending at the surface like dislocations or planar faults ending at the surface. In this case we can imagine that "surface quenching" prevents annealing of bulk defects too.

Fig. 8 shows for several temperatures, $\Delta R/R$ vs $\hbar\omega$ for a 19 Å deposit corresponding to the experiments of fig. 3. The annealing from T = 125 K was carried out at a rate of $\sim$ 2 K/minute. Fig. 8 clearly displays the progressive decay of surface plasmons excitation

with increasing temperature. The remaining structures on the Δ R/R curve for T = 253 K are just from a size effect due to the larger thickness created by the silver deposit (the silver film is not thick enough to be opaque in the spectral region near the plasma frequency This will become apparent from calculations which will be reported in the next paragraph. We conclude that the additional surface roughness induced by the quenched surface deposit completely disappears with annealing. A similar behaviour is observed on annealing of thicker layers as shown in fig .9 for a superficial deposit of 158 Å. In fig. 10 we have represented Δ R/R at 3.55 eV as a function of temperature for the experiments reported in fig. 8 and fig.9. The chosen frequency (3.55 eV) corresponds to the minimum of the Δ R/R curves due to surface plasmon excitation. In fig. 10, we have also reported unpublished experiments by Chauvineau (47) indicating a irreversible d.c resistance changes during annealing of a 80 Å thick Ag layer deposited at T=120 K on a 270 Å thick silver substrate prepared at room temperature in a similar way as our samples. The corresponding resistance changes during annealing at 3 K/minute, are given in ohms on the right ordinate scale of fig. 10. We notice that the large changes of Δ R/R do not occur at the same temperature for both layers, indicating a thickness dependence of the annealing characteristics.

The resistance changes are probably due to :

i) a decrease of the importance of the defects in the bulk of the superficial layer

i.i) a decrease of surface roughness.

The shape of the resistance curve variations is essentially the same as that of the reflectivity variations for a 158 Å deposit displaying rapid variations at about 225 K, probably indicating that at this temperature the metal is quickly organized and at the same time that

its surface is flattened out. On fig. 10 we have also represented the SERS intensity of the 1006 cm^{-1} breathing vibration mode of pyridine for a Ag surface exposed to 1L of pyridine during annealing of a "cold film" reported by Pockrand and Otto (46). The laser wavelength employed for the Raman experiments was 514 Å. Fig.10 displays a correlation between the three parameters (ΔR/R, d.c resistance and SERS peak) : the SERS peak has its maximum in the negative slope of both the other curves ; but we cannot settle an evident relationships between them.

V - NUMERICAL CALCULATIONS

Untill now we have discussed the experimental results in a rather qualitative way, sometimes indicating that numerical calculations to be presented in this paragraph corroborate our interpretations. An accurate calculation of the effects due to important roughness is a difficult task which cannot be achieved without heavy computations. To shine our results we have chosen a second order theory developed by Kröger and Kretschmann (3), which gives in our case simple formulas for the roughness induced modifications of the specular reflectivity. Kröger and Kretschmann employ a perturbative theory which is essentially the same as the Rayleigh method. Therefore it is expected to be correct for roughness heights S much smaller than the wave length and for very small slopes only. We do not know whether the latter condition is always verified in our case, but we think that this approach should be acceptable at least qualitatively.

Kretschmann and Kröger (49) consider the roughness $S(\vec{x}) = S(x,y)$ as a statistical disturbance of a plane with an average value $\langle S \rangle = 0$ and with a Fourier transform

$$s(k) = \frac{1}{(2\pi)^2} \int d^2\vec{x}\ S(\vec{x})\ e^{-i\vec{k}.\vec{x}} \qquad , \vec{k} = (k_x, k_y)$$

A normalized correlation function G (x) is defined by

$$G(\vec{x}) = \frac{1}{S'^2_F} \int_F d^2\vec{x}'\ S(\vec{x}')\ S(\vec{x}' + \vec{x})$$

with a Fourier transform :

$$g(\vec{k}) = (2\pi)^2 \cdot \frac{1}{\langle S^2 \rangle F} \left| s(\vec{k}) \right|^2$$

Where F is a very large integration area.

It was demonstrated in ref (49) that by taking statistical averages of the functions employed in the problem at hand, considering $g(\vec{k})$ independant of the $\vec{k}$ direction and some other approximations to obtain the electromagnetic fields at the surface, the reflection and transmission coefficients r and t at normal incidence for a rough metal of dielectric constant ε in contact with vacuum are given by :

$$\begin{aligned} r &= r_o \left[1 - 2 (\omega/c)^2 \langle S^2 \rangle \left(\sqrt{\varepsilon} + (1 - \varepsilon) Q \right) \right] \\ t &= t_o \left[1 + (\omega/c)^2 \langle S^2 \rangle (1 - \sqrt{\varepsilon})^2 \left(1/2 - (\sqrt{\varepsilon} + 1) Q \right) \right] \end{aligned} \qquad (4)$$

where $Q = \int dk.k\ g(k).\ \pi\ w(k)$

$w(k) = w_p(k) + w_s(k)$

$$w_p(k) = \frac{c}{\omega} \cdot \frac{k_1 k_2}{\varepsilon k_2 + k_1} \quad \text{and} \quad w_s(k) = \frac{\omega}{c} \cdot \frac{1}{k_2 + k_1}$$

where $k_1 = \sqrt{\varepsilon (\omega/c)^2 - k^2}$ and $k_2 = \sqrt{(\omega/c)^2 - k^2}$ are the wave vector components normal to the surface in the metal and in the vacuum respectivelly and

$$r_o = \frac{1 - \sqrt{\varepsilon}}{1 + \sqrt{\varepsilon}} \quad \text{and} \quad t_o = \frac{2}{1 + \sqrt{\varepsilon}}$$

are the reflection and transmission coefficients for a flat surface (that is to say with $\langle S^2 \rangle = 0$).

We see that Q can reach important values when the $w_p(k)$ denominator vanishes, that is to say for $k_1/k_2 = -\varepsilon$, which is the condition for surface plasmon excitation. The resulting effect is modulated by the surface

function k.g(k) describing the roughness topography.

In our calculations, we have used a geometry indicated in the inserts to the computed curves figures, taking into account the finite thickness of the substrate and the possible different optical constants of the overlayer. We have employed the thin film formulas for a two layer system with flat surfaces, but using for the reflection and transmission coefficients at the metal/vacuum interface eqs. (4) rather than the coefficients r_o and t_o corresponding to a flat surface.

In the present calculations surface roughness was approximated by a gaussian correlation function $G(\vec{x}) = \exp(-\vec{x}^2/\sigma^2)$ with a Fourier-transformed correlation function $g(k) = \frac{\sigma^2}{4\pi} \cdot \exp(-\sigma^2 k^2/4)$. This choice is very often employed for statistical roughness. Summarizing, in our model we consider : the finite thickness of the substrate layer (about 0.1 μm), the thickness of the superficial deposit (varing from one to one hundred monolayers), both values being determined from the microbalance frequency shift, the optical constants of the Ag substrate assumed to be those of the bulk material, those of the superficial layer which will be sometimes modified to take into account a different crystallographic structure and, finally, the roughness parameters : the mean square height of roughness $\langle s^2 \rangle$ and the correlation length σ.

We have already indicated that the negative minimum at ∿ 3.9 eV and the maximum at ∿ 4 eV are not related to roughness. Fig. 11 shows the computed values of ΔR/R vs. ħω for a superficial layer 57 Å thick having the bulk silver optical constants and a superficial roughness ($\langle s^2 \rangle = 900$ Å^2 and $\sigma = 1000$ Å) deposited on Ag substrates 10^3 Å thick and infinitely thick. It is clearly apparent that the finite thickness of the substrate is responsible for the pronounced minimum at about 3.9 eV. At this frequency silver is highly transparent and the reflectance is strongly dependent on the sample thickness.

It is not possible to compare the computed and experimental values of $\Delta R/R$ for this energy because we do not know how to accurately compute the unwanted reflection at the fused silica-copper sample holder. We have shown in fig. 11 the calculated values of $\Delta R/R$ for a flat surface, demonstrating that in this case the minimum at 3.9 eV is always present and thus clearly indicating that it is due to a size effect. It is also apparent from this figure that the minimum at 3.4 eV is due to surface roughness. This absorption is produced by surface plasmon excitation, related to the high values of $w_p(\omega)$ at this frequency. It should be underlined that the surface plasmon absorption at 3.4 eV is peaked at the same frequency independantly of the substrate thickness, its intensity being only very slightly dependant on the substrate thickness.

To give an idea of the possible influence of different dielectric constants of the surface deposit due to a poorer crystallographic structure than that of bulk silver we have computed in fig. 12 $\Delta R/R$ for a substrate 1000 Å thick and a superficial layer 57 Å thick ($\langle s^2 \rangle = 900$ Å^2, $\sigma = 600$ Å) modifying the optical constants of the surface layer in two ways :

i) dividing by two the experimental value of the mean free path of the conduction electrons for well annealed Ag films (45) (this is equivalent to an increase of the imaginary part of the Drude dielectric constant)

i.i) besides this reduction of the mean free path of free electrons, shifting by 65 meV (corresponding to 50 Angstroms on the wave length scale) in order to lower the energy of the Ag absorption edge.

To perform the later calculation we needed the interband contribution ε^b to the dielectric constant . This was obtained by substracting the Drude contribution ε^f of well annealed films from the experimental values of the dielectric constant. Then ε^b was rigidily shifted by 65 meV towards lower energies. This rather arbitrary choice was dictated by the observed absorption edge shift with disorder (50). It is not our aim

here to investigate the effect of the optical constants on the line shape around the plama frequency but rather to show their small influence on the roughness characteristic structures. We notice that the surface plasmon absorption is nearly independent of dielectric constant in contradistinction to the structures near 4 eV. This dependence on the optical constants might explain the structures observed at about 4 eV in experiments reported in fig. 3,4,5,8 and 9.

Let us notice now that the surface plasmon absorption intensity is proportional to $\langle s^2 \rangle$ and that the spectral position and width of the resonance, depend on the roughness correlation length σ. To estimate the roughness correlation length in our experiments we have computed in fig. 13 $\Delta R/R$ vs. $\hbar\omega$ for a substrate layer 1000 Å thick and a surface deposit of 57 Å (corresponding to one of the experiments of fig. 5) taking for the substrate and for the surface layer the bulk Ag optical constants, with $\langle s^2 \rangle$ = 900 Å^2 and σ = 100, 300 and 1200 Å. Comparing fig. 13 with the experimental results reported in fig. 4 corresponding to deposits on substrates at room temperature, we can conclude that for these experiments σ is approximately 100 Å. comparing now the experimental results reported in fig. 5 with fig. 12 and 13, we see that σ is rather $\sim$ 500 Å. The same value can be estimated for σ from the experiments reported in fig. 3. From our experiments it appears that σ increases with the surface plasmon absorption intensity , that is to say with $\langle s^2 \rangle$. On comparing fig 12. and fig. 5 we see that the calculated value of the intensity of the surface plasmon minimum is only one third of the experimentally found value. We roughly estimate that in this case $\sqrt{\langle s^2 \rangle}$ should be about 50 Å (the optical absorption is nearly proportional to $\langle s^2 \rangle$, as it can be seen in eq.(4)). We conclude from our experiments to a rapid increase of roughness with thickness for the thinner layers, the increase being much slower for thicker layers.

The calculations reported in fig. 14 are to be compared to the annealing experiments of fig. 8 from the shapes of the curves it can be concluded that, for a 19 Å thick deposit, annealing completely suppresses the surface plasmon excitation existing at 125 K. Thus

annealing apparently leads to roughness disappearance, i.e to a smooth surface. The positive peak at 4 eV, that we observe for experiments at the coldest temperatures in fig. 8, is due to a worse crystallographic structure of the surface layer, that completely disappears in the curve measured at 293 K. It is possible to account for this by modifying the dielectric function of the surface layer as it was explained before (fig. 12), but it is not the aim of our calculations.

VI- VERY ROUGH Ag SURFACES

In the preceding sections, we were mainly interested in the first stages of roughening of a Ag surface by quenching silver deposits paying attention to small coverages. Here we will investigate some of the characteristics of very thick deposits ($\simeq$ 1000 Å) that is to say very rough surfaces. These surfaces are particularly interesting because they present a very strong SERS for adsorbed molecules. One of the difficulties encountered in the study, the roughness relevant to SERS on these surfaces, is that it completely disappears when they are warmed up to room temperature. To our knowledge, there does not exit any reported "in situ" electron microscope studies of such films, therefore their structure is poorly known.

We have indicated that adsorbates can prevent the motion of surface atoms during annealing, maintaining a roughness which would otherwise be suppressed by increasing the temperature. This effect was experimentally demonstrated by us with Al and Cu adsorbates subsequently oxidised and is employed as a means to investigate the surface of rough quenched films. Let us describe now one of our experiments. We prepare first, at room temperature, in a vacuum better than 10^{-9} torr, a silver film 600 Å thick, and then we cool the sample untill the temperature is stabilized to 153 K. In the different experimental runs we obtain limiting temperatures differing by approximately 10 K. This

is probably due to the quality of the thermal contact between each glass plate and the sample holder. Then we evaporate 1470 Å of silver on the sample maintained at 153 K followed by the evaporation of 5 Å on one half of the sample. The sample is then exposed to 45 L (1 L = 10^{-6} torr X 1 sec.) of O_2, finally it is brought up to room temperature at a rate of about 2 K/min . The effect of the Al deposit, subsequent oxygen exposure and annealing was followed by spectral measurements of $\Delta R/R$. Fig 15 shows electron microscope micrographs of carbon replicas made at room temperature by evaporating C at an angle of incidence of 45 degrees after having taken the sample out of the vacuum chamber. Fig. 15a corresponds to the surface without the Al deposit and fig.15b to the Ag surface covered by the Al surface layer. On fig. 15a the grain boundary ripples are clearly visible but otherwise the surface appears rather smooth. On fig. 15b an important roughness is apparent, with a quasi-period of 200-300 Å closely related to the correlation length. It must be underlined that the surface roughness seen in the micrograph of fig. 15 b is maintained by the Al oxyde and is not an effect of the oxyde itself. It could be argumented that the Ag surface not covered by Al is also exposed to the oxygen atmosphere and therefore a similar effect should be observed. The possible roughness induced by oxygen on silver is in any case much smaller than the one due to the Al oxyde, as can be seen from fig. 15, probably because of the very low sticking coefficient of oxygen on silver (6.10^{-4} at room temperature (51)). We have performed equivalent experiments with superficial Cu layers exposed to oxygen and we have found similar results. In conclusion, it appears that we can maintain, at room temperature, an important roughness existing on quenched silver films, just by covering the surface with a very thin surface layer.

We will now examine the point, actually discussed, from an optical point of view with differential reflectivity measurements. The continuous curve (labelled I) on fig.16 shows $\frac{\Delta R}{R} = 2(R'-R)/(R'+R)$ between the clean Ag surface (R) and the surface covered with the Al oxyde (R') for the experiments reported in the discussion of fig. 15. We found the pronounced minimum at 3.9 eV corresponding to the small values of R as indicated

in section III, but two additional minima at about 2.1 eV and 3.2 eV are also apparent. A first interpretation of this absorption would be to assign the structures at 2.1 and 3.2 eV to optical transitions between electronic states of this system, in other words to an optical absorption due to the surface layer. Following the discussion of the problem at hand, we will [illegible] that both minima are due to absorption induced by surface roughness. In fig. 17 we have reported experiments analogous to those of fig. 16 (a Ag deposit 1830 Å thick [illegible] and a superficial deposit of Cu 2.4 Å thick) after 150 L of O_2. The curve labelled I corresponds to $\Delta R/R$ between bare silver and silver covered by the Cu deposit plus 150 L of O_2. We see two absorptions similar to those of fig. 16 at nearly the same energies. It would be very unlikely that absorptions induced by optical transitions on the adsorbate should display a very similar structure for both adsorbates.

If we examine now the $\Delta R/R$ variations during annealing represented by discontinuous curves in fig. 16 and 17, we notice that in both cases the absorptions originally located at about 2 and 3 eV progressively shift and grow with decreasing temperature, a fitting indicating that they are not absorptions characteristic of the adsorbate but of the surface itself. In particular, for high temperatures (for instance T= 275 K in fig. 16) we are comparing two Ag surfaces with quite different roughness (fig. 15a and b) which give rise to large values of $\Delta R/R$ ($\sim$ 30 %) obviously not due to the superficial layer itself.

We can inquire whether one or both absorptions are due to a bulk effect. This is certainly not the origin of the highest energy absorption which is progressively shifted with annealing to the surface plasmon frequency reaching a deep minimum similar to the one seen in fig. 5. Having in mind the reported interpretation of the optical absorption of quenched Ag films (52) we can ask about the origin of the low energy minimum. We can imagine that during annealing the film portion which is not covered by the surface layer is acquering a more perfect crystallographic structure leading to different optical constants with corresponding changes in the reflectivity. Moreover Hunderi (52) assigns the

anomalous
/absorption of Ag films to bulk defects in the films, which behave as a composite medium with two dielectric constants having a resonant frequency. In the present case, we can argue that this is not the reason for the observed absorptions, because they are continuously shifting away from the absorption of the unannealed film, which is only a surface phenomena. It is clear that if bulk defects had a resonant frequency it should be completely independent of surface absorptions. It must be considered that the structures in fig. 16 or 17 are unambiguously assigned to the surface. For instance, the reflectivity structures seen in fig. 17 for a Cu monolayer (curve II) are modified with exposure to 150 L of oxygen. The present experiments can be understood as due to roughness induced enhanced electromagnetic fields at the surface in the same way as electromagnetic fields are enhanced at the surface plasmon excitation experiments with a grating or an attenuated total reflection coupler. For a plane wave imping on a flat surface the electromagnetic field seen by a surface molecule, is a smooth function easily deduced from the optical constants of the metal, but for a rough surface the field at the surface is not easily known and can have large values for specific spectral regions. This is what probably happens in our experiments. From this point of view, the optical absorptions at $\sim$ 2 eV and $\sim$ 3 eV in fig. 16 and 17 correspond to high electromagnetic fields at these frequencies. The same argument can be put forward in order to explain the observed modifications during annealing. We are comparing a rough surface having pronounced electromagnetic resonances with an other which becomes more and more flat with the corresponding vanishing of the resonances. It is not our aim here to discuss the enhancement of electromagnetic fields at rough surfaces, but only to point out that it must be taken into account for spectroscopic studies on rough surfaces. We have already reported a comparative study of submonolayer optical absorption on rough and flat Ag surfaces allowing us to determine the average local field at the surface (14). In our opinion, the low frequency absorption is due to localized plasmons at the surface protuberances and the high frequency absorption corresponds to a propagating

mode which, for a flat surface, [illegible] usual surface plasmon mode. We think that annealing, even for covered film, leads to a smoothing of the sharp protuberances still maintaining a large roughness. In fig. 16 and 17 we can imagine that this effect is more important for Cu that for Al ; at high temperatures, the shoulder at ~ 3 eV has nearly disappeared for the Cu oxyde. Taking for a surface bump a model of a prolate hemispheroid on a conducting plane, a resonance at 2 eV is found on Ag for a ratio of the major to the minor axis equal to 3 (9) shifting to higher energies as this ratio decreases, up to 3.2 eV for a sphere. As the annealing shifts the [illegible] energy, we can imaginate that what is happening is a flattering of the surface bumps during annealing. At present, we cannot conclude about this hypothesis.

To check our conclusion, which assigns the observed absorption to surface roughness and not to bulk defaults, we have performed a different kind of experiments. The idea is that if this absorption is due to surface roughness it should not be observed in reflectivity measurements performed from the back side of the fused silica substrate. In the standard configuration described above, we cannot measure the reflection through the fused silica, because of the copper cooling block, but, with a minor modification, we have overcome this difficulty with the restrictive condition that absolute values of reflectivity and temperature cannot be known. Because we are interested in a comparative study, this restrictions will not be crucial for obtaining the supplementary information sought for.

We have proceeded as follows :

a glass plate longer that the cold holder is fixed on it. By a 180 ° rotation of the sample, we can present nearly either the vacuum side of the silver film or the glass side in front of the optical window. A schematic representation of the experimental geometry is indicated in fig. 18. Relative values of the reflectivity, i.e reflectivity multiplied by an apparatus factor, are obtained using the double beam spectrophotometer described in section II. The temperature (~ 140 K) is known on the sample side in contact with the holder, but not on the unsupported end.

mode which, for a flat surface, becomes the usual surface plasmon mode. We think that annealing, even for covered film, leads to a smoothing of the sharp protuberances still maintaining a large roughness. In fig. 16 and 17 we can imagine that this effect is more important for Cu that for Al ; at high temperatures, the shoulder at ∿ 3 eV has nearly desappeared for the Cu oxyde. Taking for a surface bump a model of a prolate hemispheroid on a conducting plane, a resonance at 2 eV is found on Ag for a ratio of the major to the minor axis equal to 3 (9) shifting to higher energies as this ratio decreases up to 3.2 eV for a sphere. As the annealing shifts the lower energy resonance to higher energy, we can imaginate that what is happening is a flattering of the surface bumps during annealing. At present, we cannot conclude about this hypothesis.

To check our conclusion, which assigns the observed absorption to surface roughness and not to bulk defaults, we have performed a different kind of experiments. The idea is that if this absorption is due to surface roughness it should not be observed in reflectivity measurements performed from the back side of the fused silica substrate. In the standard configuration described above, we cannot measure the reflection through the fused silica, because of the copper cooling block, but, with a minor modification, we have overcome this difficulty with the restrictive condition that absolute values of reflectivity and temperature cannot be known. Because we are interested in a comparative study, this restrictions will not be crucial for obtaining the supplementary information sought for.

We have proceded as follows :

a glass plate longer that the cold holder is fixed on it. By a 180 ° rotation of the sample, we can present nearly either the vacuum side of the silver film or the glass side in front of the optical window. A schematic representation of the experimental geometry is indicated in fig. 18. Relative values of the reflectivity, i.e reflectivity multiplied by an apparatus factor, are obtained using the double beam spectrophotometer described in section II. The temperature (∿ 140 K) is known on the sample side in contact with the holder, but not on the unsupported end.

In the first experiment on a cold substrate, a 1660 Å thick silver film is deposited on the unsupported side of the sample and the reflectivity is measured first at this unknown temperature and then, after annealing, at room temperature. The sample is extracted from the vacuum chamber and absolute values of reflectivity are measured with a Cary 14 spectrophotometer. Assuming that these values correspond to those of the relative reflectivity at this room value for the sample at room temperature, a calibration function of the apparatus is obtained. Fig. 18 shows the calibrated values of the reflectivity from the vacuum side at low temperature (curve A) and at room temperature (curve B). In a second experiment, we have deposited 1800 Å of silver on the cooled substrate and we have measured the reflectivity from the glass side at low temperature (curve C) and at room temperature (curve B). We have assumed that the reflectivity at room temperature is the same for both experiments. We did not take into account the multiple reflections in the glass plate and the difference in the refractive index n of the medium in contact with silver at the reflecting interface (vacuum n=1 or glass n=1.5). It is clear that in the present experiments we cannot expect to obtain accurate values of the reflectivity, but the relative values of curves A and B and curves A and C should be at least qualitatively good. This is the interesting point in our discussion. For $\hbar\omega$>2eV curve B takes higher values that curve A. This is probably a real fact and not an artefact of our experimental set-up. At low temperature, roughness has a small correlation length producing little scattered light. When the sample is warmed up the roughness becomes "wavier" with a large number of short Fourier components and the amount of scattered light increases with a corresponding reflectivity loss. The increase of s and p-polarized scattered light with annealing of equivalent quenched films was clearly shown by Pettenkofer (53).

Although, these measurements are not very accurate, the comparative values for each experiment with temperature should be significant

suggesting that on the vacuum side a supplementary absorption exists besides the surface plasmon excitation. The differences found between curve C and B are probably due to different values of the optical constants only. This confirms the interpretation given for the annealing curves (fig. 16 and 17).

CONCLUSION

From the experimental point of view, we have clearly shown that spectroscopic differential reflectivity is a very powerful tool for surface studies. It allows the measurement of electronic modifications of an interface induced, for instance, by atomic or molecular adsorption or, as in this paper, to investigate the electromagnetic properties of a surface.

We have thoroughly developed an investigation on the early roughening of a clean silver surface by depositing various thicknesses of silver overlayers. When the silver substrates are cooled to 140 K, measurable values of $\Delta R/R$ are found even for a monolayer coverage only. The observed structure, probably due to the electronic properties of surface defects on the atomic scale, are not yet clearly understood by us. For thicker deposits, a well defined absorption at $\sim$ 3.6 eV due to surface plasmon excitation is found. Experimental evidence of a roughness induce splitting of surface plasmons is given for various thicknesses of the deposited silver and the experiments are compared with theory. A large amount of theoretical work was already devoted to this subject, but only few experimental results were reported.

For extremely rough silver films we noticed the appearence of an optical absorption at about 2.5 eV due to surface roughness. We conclude that differential reflectivity experiments can be successfully employed to investigate electromagnetic resonant phenomena other than surface plasma waves, which are actually well known. Specific studies concerning the surface modes are not widely generalized and we indicate how such studies can be performed, in particular by using a superficial oxide layer, to fix the surface roughness existing at low temperature on quenched metal films.

REFERENCES

1. A.A. MARADUDIN in Modern Problems in [illegible] Physics, Vol. 11 Surface Polaritons Ed. V.M. Agranovich and D.L. Mills p. 405, North-Holland Publishing 1982.

2. H. RAETHER, in ref. 1, p. 331.

3. E. KRÖGER and E. KRETSCHMANN, Z. Phys. 237, 1 (1970).

4. N. GARCIA, To be published in Optics Comm. (45, 1983).

5. A.A. MARADUDIN and N. GARCIA, To be published in Optics Comm. (45, 1983).

6. D.W. BERREMAN, Phys. Rev. 163, 855 (1967).

7. D.W. BERREMAN, Phys. Rev. B1, 381 (1970).

8. R. RUPPIN, Sol. State Comm. 39, 903 (1981).

9. J.I. GERSTEN, A. NITZAN, J. Chem. Phys. 73, 3023 (1980).

10. M. KERKER, D.S. WANG and H. CHEW, Applied. Opt. 19, 3373 (1980).

11. J.A. CREIGHTON in Surface Enhanced Raman Scattering, Ed. by R.K. Chang and T.E. Furtak (Plenum Press, New-York) 1981, p. 315.

12. D. BEAGLEHOLE and O. HUNDERI, Phys. Rev. B2, 309 (1970).

13. O. HUNDERI and D. BEAGLEHOLE, Phys. Rev. B2, 321 (1970).

14. T. LOPEZ-RIOS, Y. BORENSZTEIN and G. VUYE, will be presented to the "International Conference on Ellipsometry and Other Optical Methods for Surface and Thin films analysis" Paris, France 7-10 June 1983.

15. U. FANO, J. Opt. Soc. Am. 31, 213 (1941).

16. A. OTTO, To appear in "Light Scattering in Solids", Vol. IV
Ed. by M. Cardona and G. Güntherodt (Springer).

17. M. FLEISCHMANN, P.J. HENDRA and A.J. McQUILLAN, Chem. Phys. Letters
26, 163 (1974).

18. J.C. TSANG, J.R. KIRTLEY, J.A. BRADLEY, Phys. Rev. Letters
43, 772 (1979).

19. A. OTTO, Surf. Scien. 75, L392 (1978).

20. T.H. WOOD, M.V. KLEIN, Sol. State Comm. 35, 263 (1980).

21. T. LOPEZ-RIOS, Y. BORENSZTEIN and G. VUYE, Journal de Physique Lett.
44, L99 (1983).

22. D. BEAGLEHOLE and E. ERLBACH, Phys. Rev. B6, 1209 (1972).

23. R.J. NASTASI-ANDREWS and R.E. HUMMEL, Phys. Rev. B16, 4314 (1977).

24. G.W. RUBLOFF, J. ANDERSON, M.A. PASSLER and P.J. STILES,
Phys. Rev. Lett. 32, 667 (1974).

25. J.A. CUNNINGHAM, D.K. GREENLAW and C.P. FLYNN, Phys. Rev.
B22, 717 (1980).

26. G.B. BLANCHET, P.J. ESTRUP and P.J. STILES, Phys. Rev. Lett.
44, 171 (1980).

27. T. LOPEZ-RIOS and G. VUYE, J. Phys. E 15, 456 (1982).

28. H. KIESSIG, Ann. Physik 10, 5769 (1931).

29. M. GANDAIS, V. NGUYEN VAN and S. FISSON, Thin Solid Films 15, 233 (1973).

30. K.L. CHOPRA, Thin Film Phenomena, McGraw-Hill 1969, p. 185.

31. S.O. SARI, D.K. COHEN and K.D. SCHERKOSKE, Phys. Rev. B21, 2162 (1980).

32. J.P. CHAUVINEAU, Surf. Scien. 93, 471 (1980).

33. J.P. CHAUVINEAU, J. of Crystal Growth 53, 505 (1981).

34. C. PARISET and J.P. CHAUVINEAU, Surf. Scien. 78, 478 (1978).

35. C. PARISET, Thèse Orsay 1976 (unpublished).

36. D. SCHUMACHER and D. STARK, Surf. Scien. 123, 384 (1982).

37. O. HUNDERI and H.P. MYERS, J. Phys. F 3, 683 (1973).

38. M. MOSKOVITS and D.P. DILELLA in ref. 11, p. 243 ;
P.H. Mc BREEN and M. MOSKOVITS, J. Appl. Phys. 54, 329 (1983).

39. T. LOPEZ-RIOS, Y. BORENSZTEIN and G. VUYE, To be published.

40. E. KRETSCHMANN, T.L. FERRELL and J.C. ASHLEY, Phys. Rev. Lett. 42, 1312 (1979).

41. R.H. RITCHIE, E.T. ARAKAWA, J.J. COWAN and R.N. HAMM, Phys. Rev. Lett. 21, 1530 (1968).

42. T.S. RAHMAN and A.A. MARADUDIN, Phys. Rev. B 21, 2137 (1980).

43. R. KOTZ, H.J. LEWERENZ and E. KRETSCHMANN, Phys. Lett. 70 A, 452 (1979).

44. N.W. WILLIAMS, J.C. ASHLEY, E. KRETSCHMANN, T.A. CALLCOTT, M.S. CHUNG and E.T. ARAKAWA, Phys. Lett. 73 A, 231 (1979).

45. M.M. DUJARDIN and M.L. THEYE, J. Phys. Chem. Solids 32, 2033 (1971).

46. M. DOYAMA and J.S. KOEHLER, Phys. Rev. 127, 21 (1962).

47. J.P. CHAUVINEAU, Private Communication.

48. J. POCKRAND and A. OTTO, Solid State Comm. 35, 1159 (1981).

49. E. KRETSCHMANN and E. KRÖGER, J. Opt. Soc. Am. 65, 150 (1975).

50. P. WINSEMIUS, Thesis Leiden University (1973).

51. M. ALBERS, W.J.J. VAN DER WAL, O.L.J. GIJZEMAN and G.A. BOOTSMA, Surf. Scien. 77, 1 (1978).

52. O. HUNDERI, Phys. Rev. B 7, 3419 (1973).

53. C. PETTENKOFER, diploma work Universität Düsseldorf 1981, see also ref. 16.

FIGURES CAPTIONS

Fig. 1 - Principle of the differential spectrophotometer. The vibrating mirror M directs the optical beam alternatively on the two halves (A and B) of the sample whose slight difference of reflectance is to be measured. The synchronous detection (S.D) and the feedback on the high voltage of the photomultiplier (PM) are also indicated. The insert shows the PM output as a function of time for a given wave-length.

Fig. 2 - The optical set-up. S_1 and S_2 are the ultraviolet and visible sources respectively. A concave mirror m_1 is used to form the image of the exit slit O of the monochromator(mono) in O' on the vibrating mirror M. The mirror m_3 is used to focus the beam on the photomultiplier PM. The sample is located at the center of the vacuum chamber. M' is a beam splitter providing a reference beam for absolute reflectivity measurements and C is the chopper used for these measurements.

Fig. 3 - $\frac{\Delta R}{R}$ at normal incidence vs. $\hbar\omega$ for 2.6, 10.5 and 19 Å of silver deposited at T=125 K on a 836 Å thick silver film. One silver monolayer corresponds to 2.35 Å. The insert represents the bulk silver reflectance.

Fig. 4 - $\Delta R/R$ at normal incidence vs. $\hbar\omega$ for 24.5 and 65.5 Å of silver deposited on 1253 Å thick silver substrate kept at room temperature.

Fig. 5 - $\Delta R/R$ at normal incidence vs. $\hbar\omega$ for various thicknesses d of the surface layer : ——— d= 19 Å ; — — d= 57 Å ; — — — d= 124 Å ; — . — d= 187 Å ; ..... d= 2000 Å on a 1000 Å thick Ag substrate kept at T = 140 K. The last curve is reduce by a factor of 3.

Fig. 6 - Part of the $\Delta R/R$ vs. $\hbar\omega$ curve of Fig. 5 shown on an enlarged scale.

Fig. 7 - Computed values of the response function $|K/n_r|^2.(c/\omega)^2$ vs. $\hbar\omega$ for $a^2 = 0, 0.05, 0.1$ and 0.2 with the bulk values of the silver optical constants. The upper scale gives the real part of the silver dielectric function.

Fig. 8 - Measured values of $\Delta R/R$ vs. $\hbar\omega$ for the 19 Å thick film studied in fig. 3 during annealing at different temperatures of the samples : —·—· T = 125 K; --- T = 173 K; —— T = 196 K; ···· T = 253 K

Fig. 9 - $\Delta R/R$ vs. $\hbar\omega$ for a 158 Å thick layer during annealing at different temperatures of the sample: ·—·—T = 145 K; — — T = 193 K; —— T = 230 K; ·····T = 260 K.

Fig. 10 - $\Delta R/R$ vs. temperature T at a fixed frequency ($\hbar\omega$ = 3.7 eV) corresponding to the maximum of the surface plasmon absorption for quenched layers 19 Å thick -•-•- and 158 Å thick —+—+— (inner ordinates scale at the left). The curve for the 158 Å thick film was reduced by a factor of 10. The d.c resistance variation of 80 Å thick silver deposit quenched at 120 K on a silver substrate 270 Å thick are also shown (——, ordinate scale at the right, after Chaurineau (47)) together with the SERS intensity of the 1006 cm^{-1} pyridine line after Pockrand and Otto (48) (outer ordinate scale at the left, - - - -).

Fig. 11 - Computed values of $\Delta R/R$ vs. $\hbar\omega$ for a superficial layer 57 Å thick with optical constants of bulk silver and a surface roughness given by $\langle s^2 \rangle$ = 900 $Å^2$ and $\sigma = 10^3$ Å on silver substrates 10^3 Å (——) and infinitely thick (— —). $\Delta R/R$ vs. $\hbar\omega$ for the same film with a smooth surface on the 1000 Å thick silver substrate is also shown (·-·-·-).

Fig. 12 - Computed values of $\Delta R/R$ vs. $\hbar\omega$ for a rough superficial layer ($\langle s^2 \rangle$ = 900 Å^2, σ = 600 Å) 57 Å thick on a silver substrate 1000 Å thick. The optical constants of the superficial layer were chosen as follows : ——— corresponds to those of bulk silver (ε); —·—·— corresponds to a factor of two reduction of the values of the relaxation time in the free electron part $\varepsilon^f(\omega)$ of the dielectric constant; — — is computed with the same values of $\varepsilon^f(\omega)$ and an overall shift of the interband contribution $\varepsilon - \varepsilon^f$ by 65 meV towards lower energies.

Fig. 13 - Computed values of $\Delta R/R$ vs. $\hbar\omega$ for a silver layer 57 Å thick on a silver substrate film 1000 Å thick both films having the bulk optical constants of silver. The surface roughness is described by $\langle s^2 \rangle$ = 900 Å^2 and σ = 100, 300 and 1200 Å. The case of a smooth surface is also represented.

Fig. 14 - Computed values of $\Delta R/R$ vs. $\hbar\omega$ for a superficial layer 19 Å thick on a substrate 835 Å thick both having the bulk silver optical constants. The roughness of the superficial layer is characterized by σ = 500 Å and $\langle s^2 \rangle$ = 225 Å^2, 100 Å^2 and 0 Å^2.

Fig. 15 - Electron microscope photographs of carbon replicas made at room temperature by evaporating C at an angle of incidence of 45 degrees : a) bare silver surface ; b) the silver surface is covered with a 5 Å aluminium layer. The bar corresponds to 10^3 Å.

Fig. 16 - Differential reflectivity $\Delta R/R$ vs. $\hbar\omega$ between a silver film 1470 Å thick quenched on a substrate at 153 K and the same covered by 5 Å of Al and exposed to 45 L of O_2. The discontinuous lines gives $\Delta R/R$ during annealing at various temperatures (indicated at the left of the curves). Each curve is shifted by 2.5 10^{-2}.

Fig. 17 - Differential reflectivity $\Delta R/R$ vs. $\hbar\omega$ between a 1830 Å thick silver film quenched on a substrate at 153 K and the same covered by 2.6 Å of Cu (curve II) and exposed to 150 L of oxygen (curve I). The discontinuous lines give the $\Delta R/R$ values during annealing at different temperatures (indicated at the left of the curves). Each curve is shifted by 10^{-2}.

Fig. 18 - Reflectivity R vs. $\hbar\omega$ at near normal incidence for a silver film approximately 1400 Å thick quenched on a fused silica plate. Curve A corresponds to measurements from the vacuum side at low temperature and curve B to the same performed at room temperature, while curve C shows the measured values of R at low temperature but from the glass side. The results shown on curves A and C were obtained on different samples. The experimental geometry is sketched in the insert.

FIG. 1

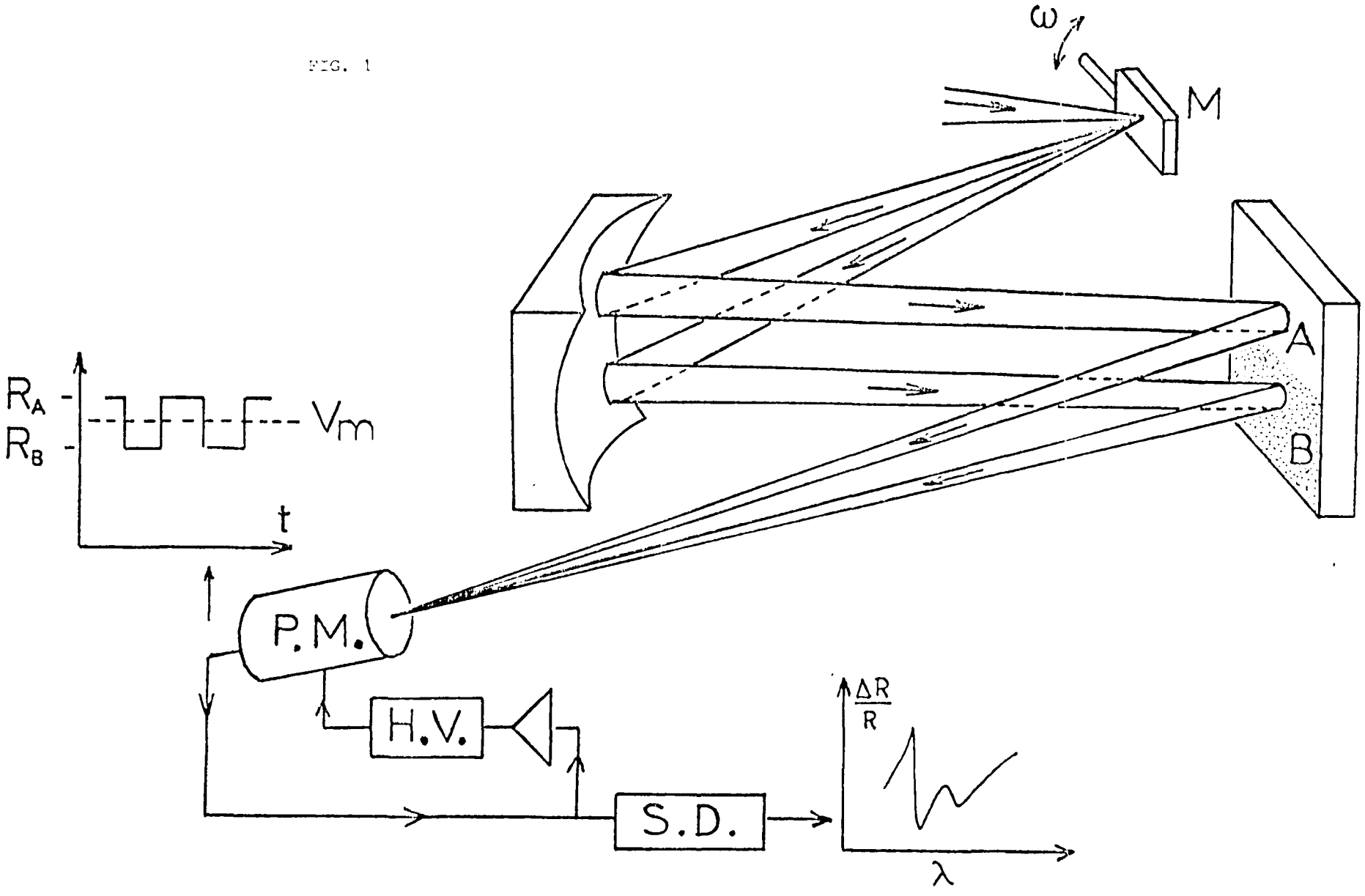

FIG.2

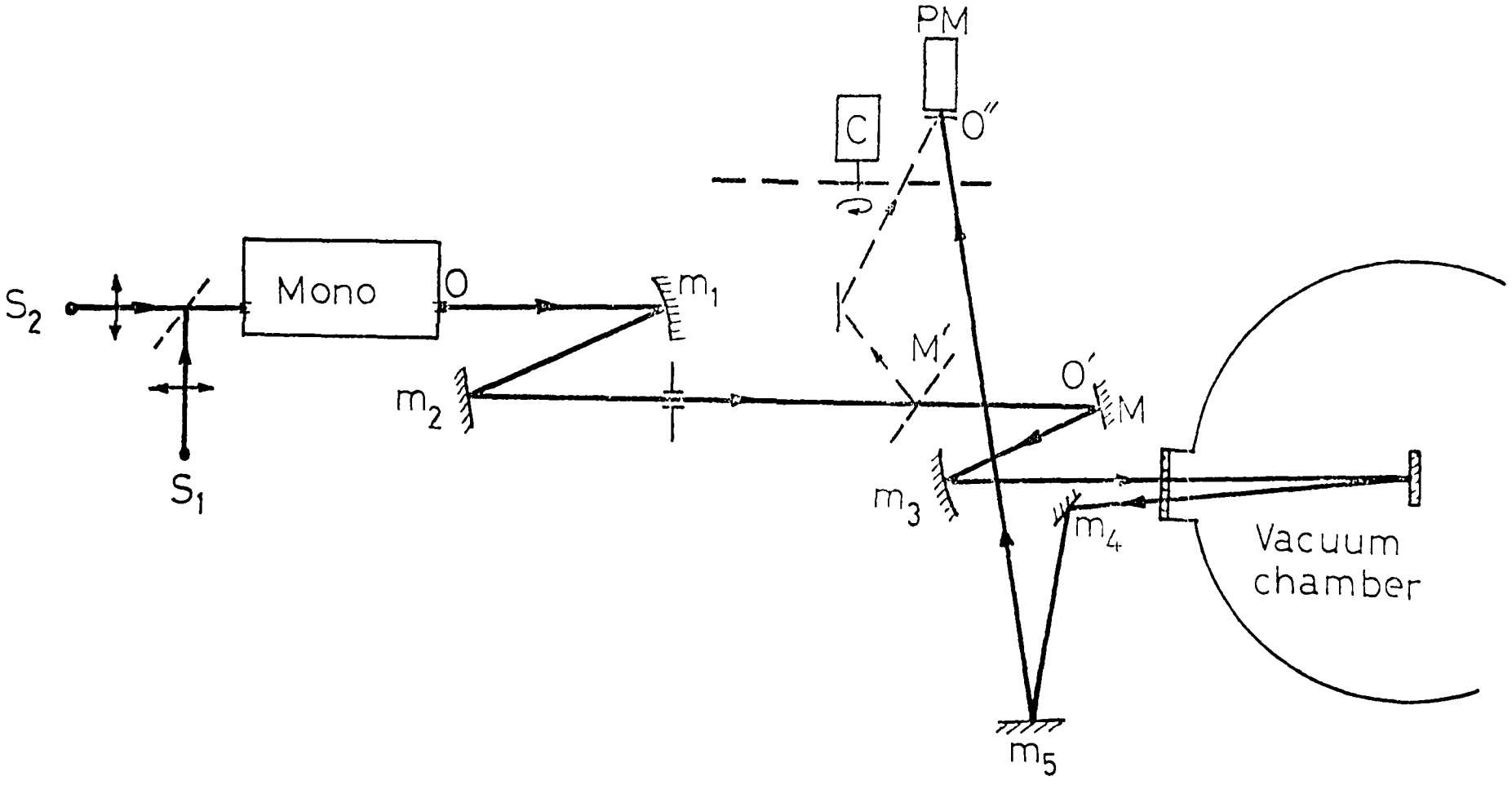

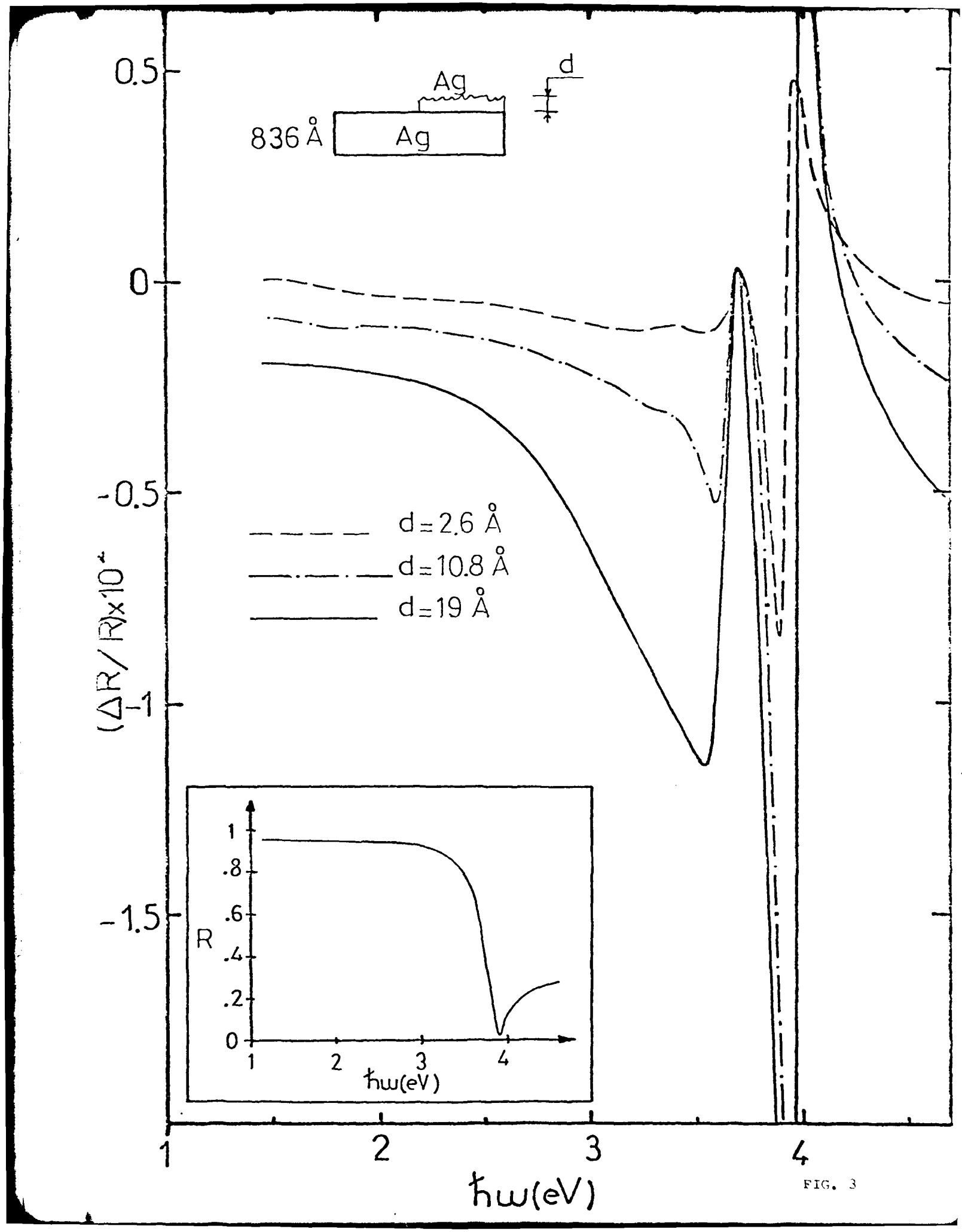

FIG. 3

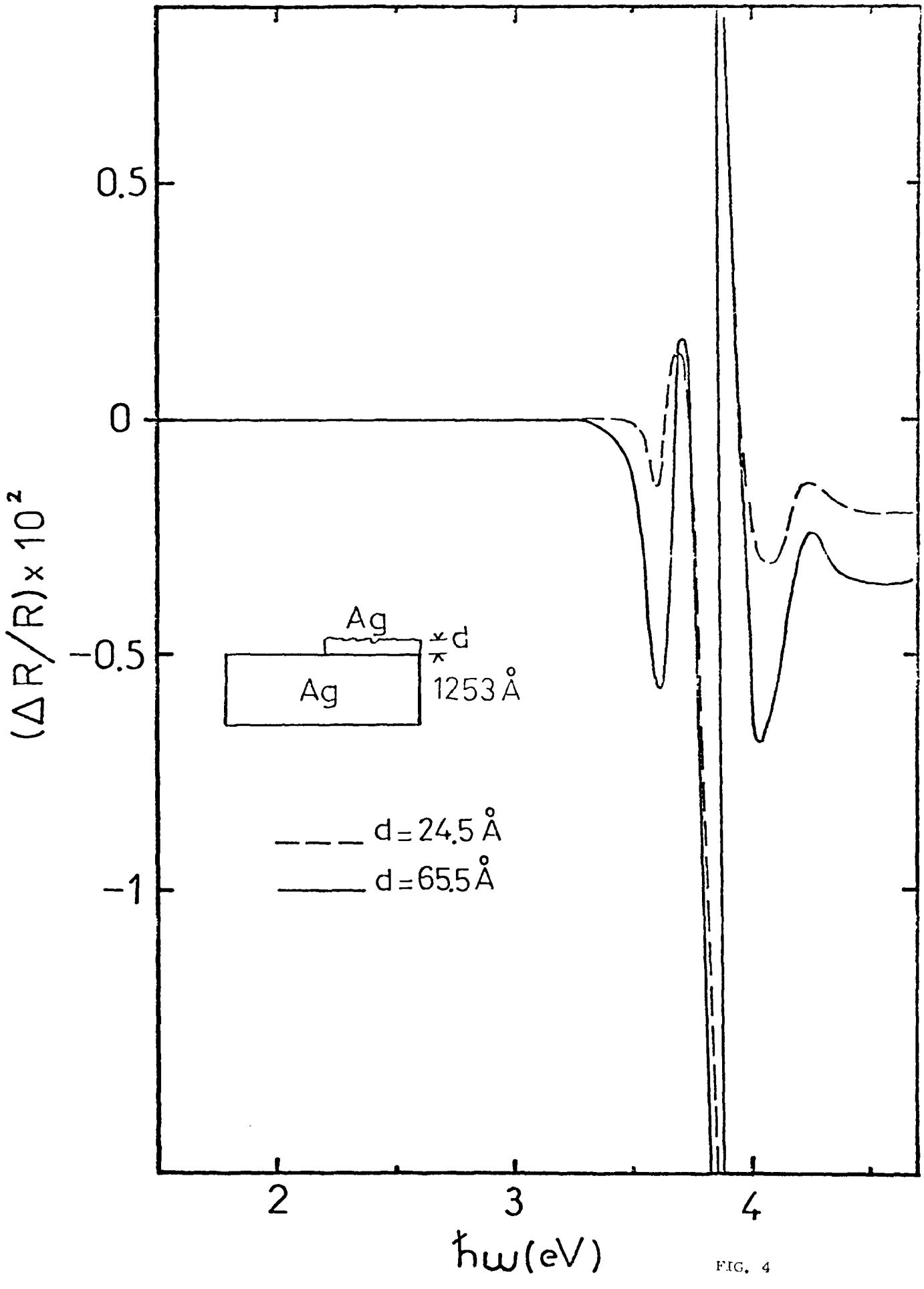

FIG. 4

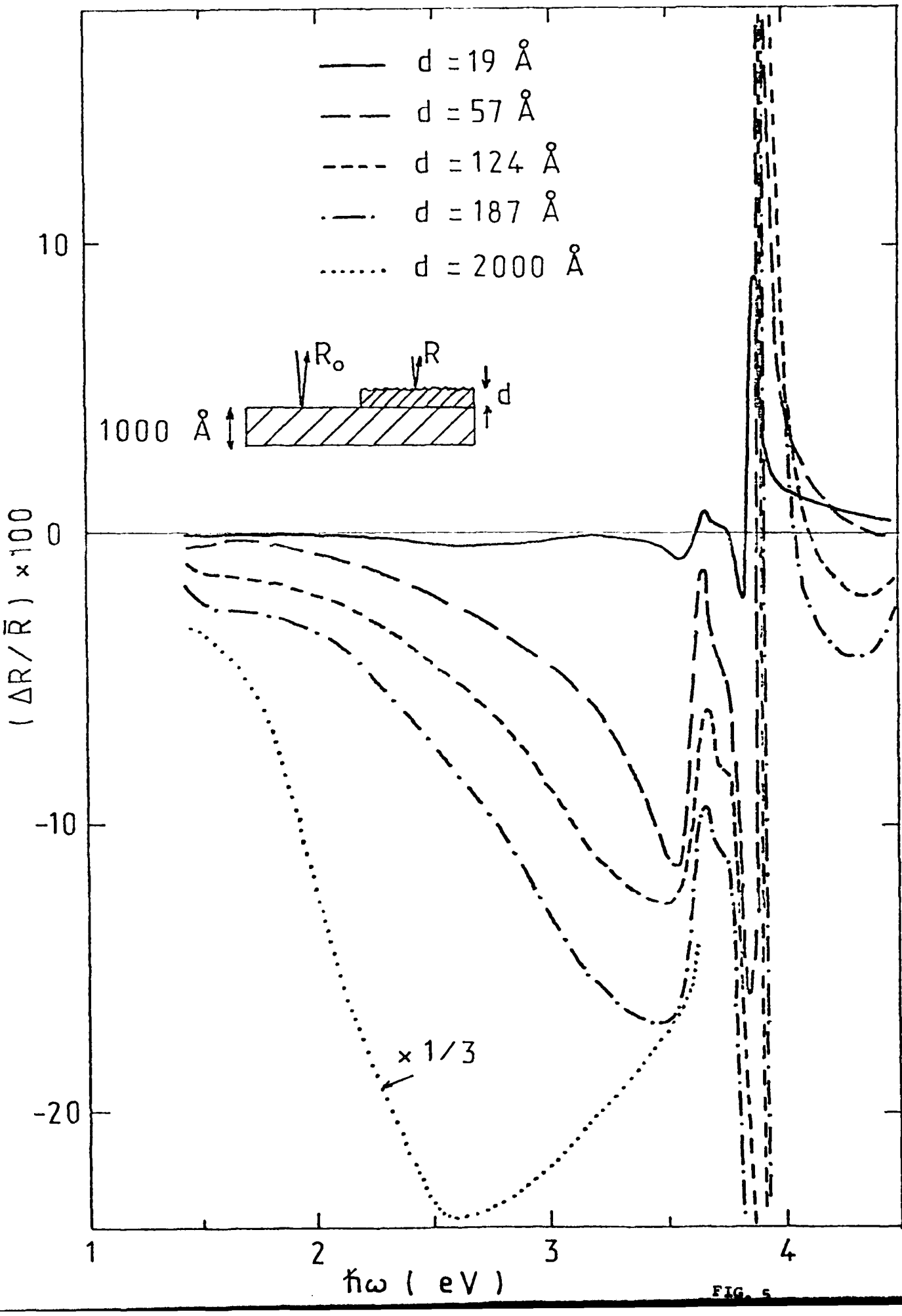
d = 19 Å
d = 57 Å
d = 124 Å
d = 187 Å
d = 2000 Å
R₀
R
d
1000 Å
10
0
-10
-20
× 1/3
(ΔR / R̄) × 100
1
2
3
4
ħω (eV)

FIG. 5

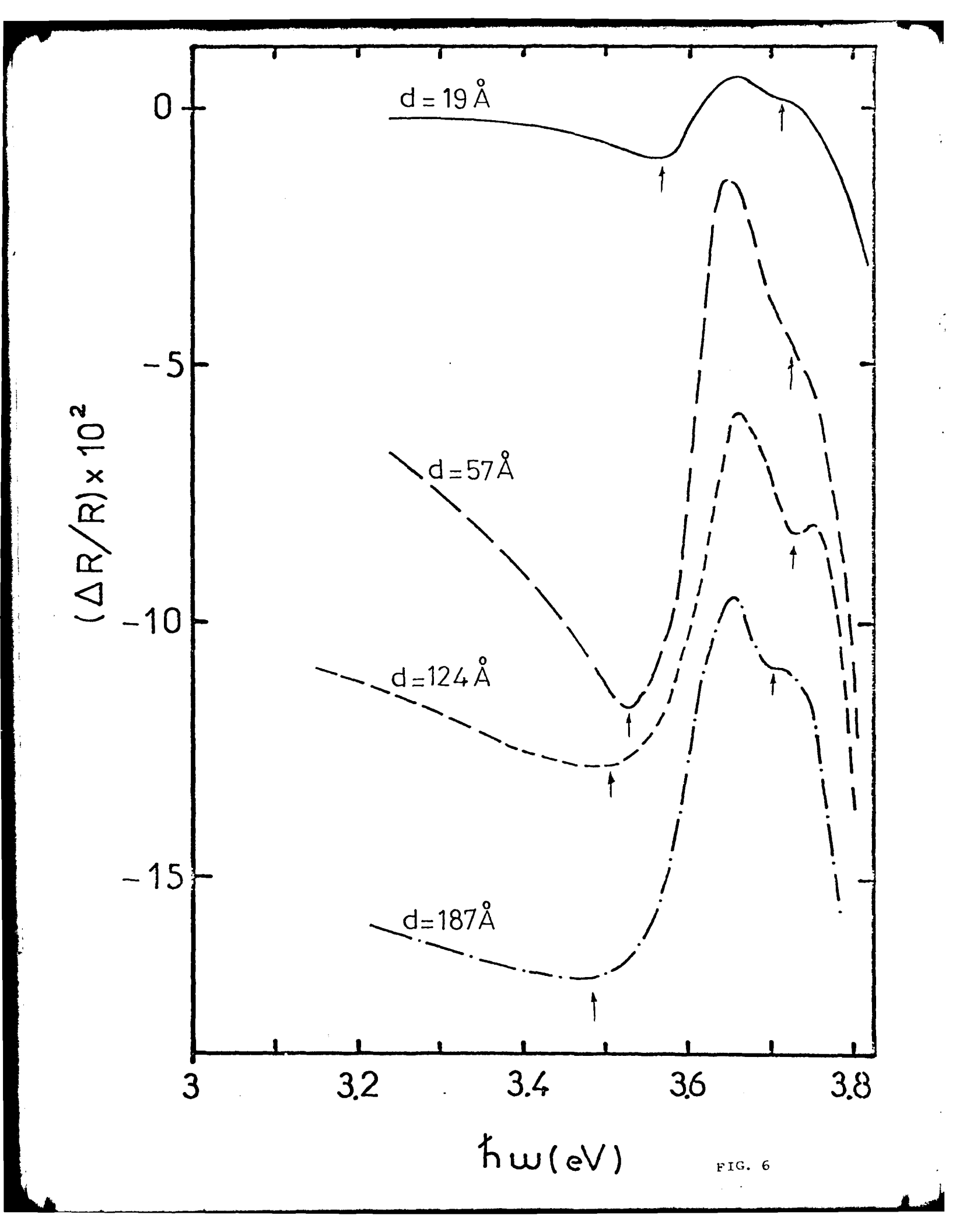

FIG. 6

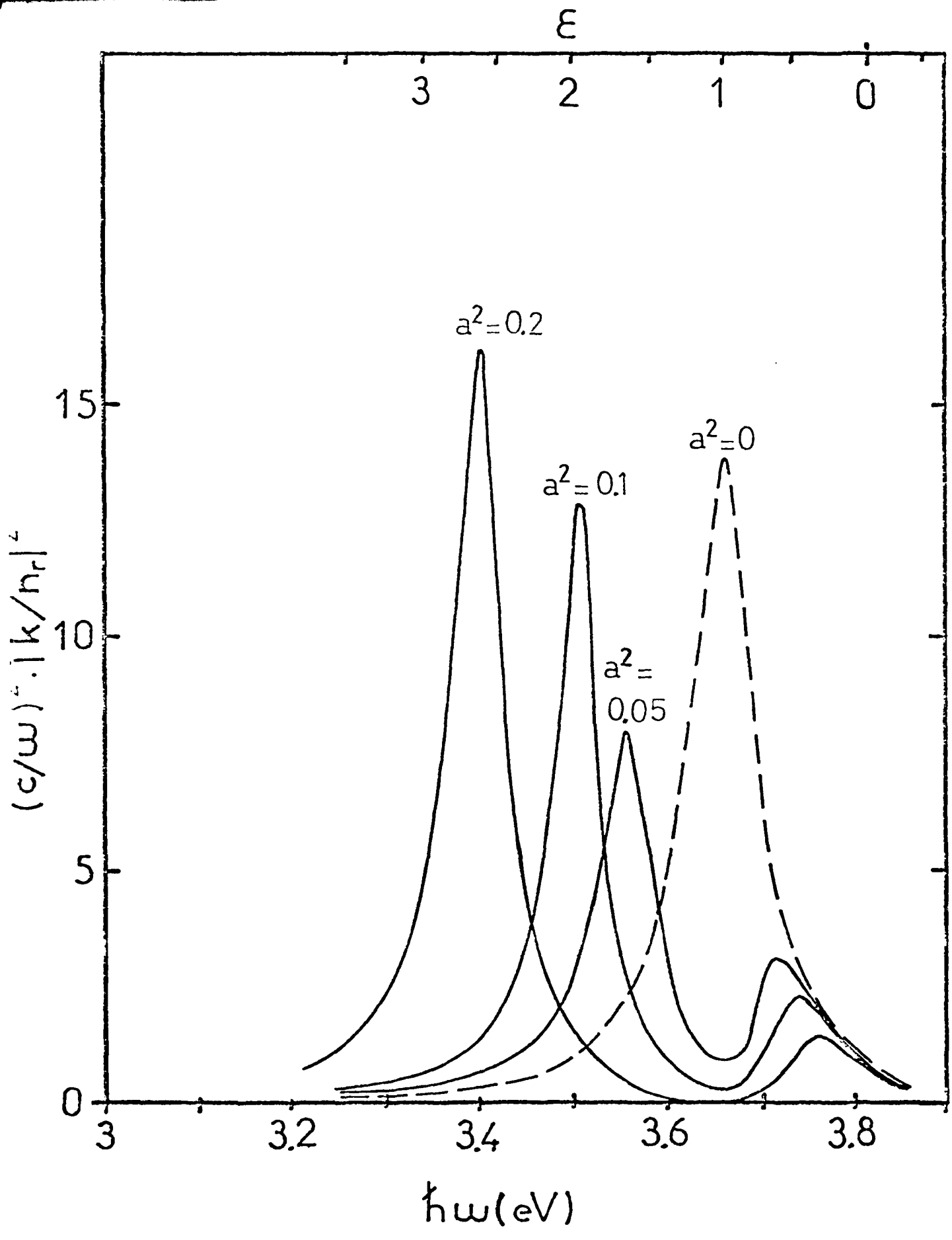
ε
3
2
1
0
$a^2=0.2$
$a^2=0.1$
$a^2=0$
$a^2=$
0.05
15
10
5
0
$(c/\omega)^2 \cdot |k/h_r|^2$
3
3.2
3.4
3.6
3.8
$\hbar\omega$(eV)

FIG. 7

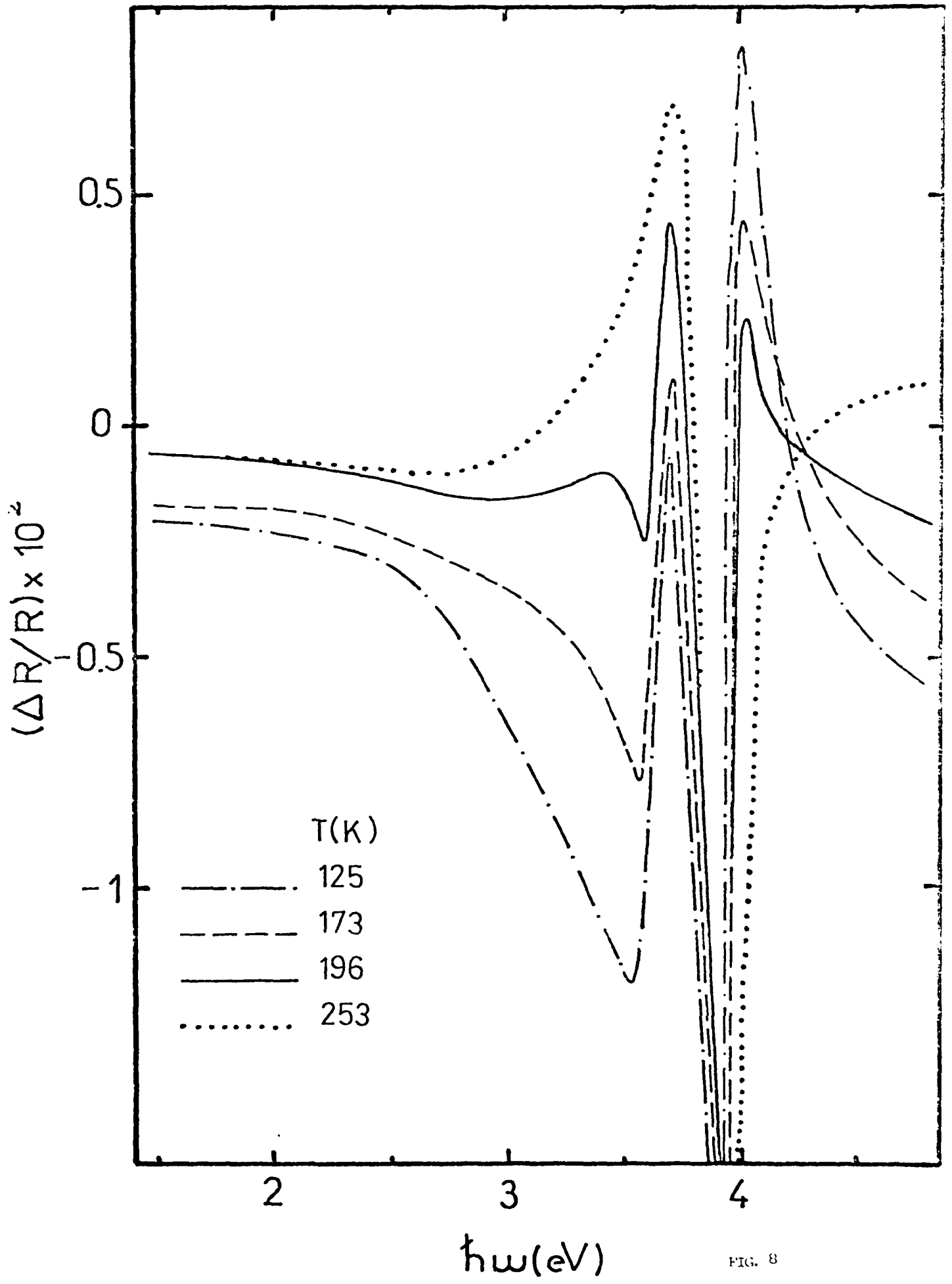

FIG. 8

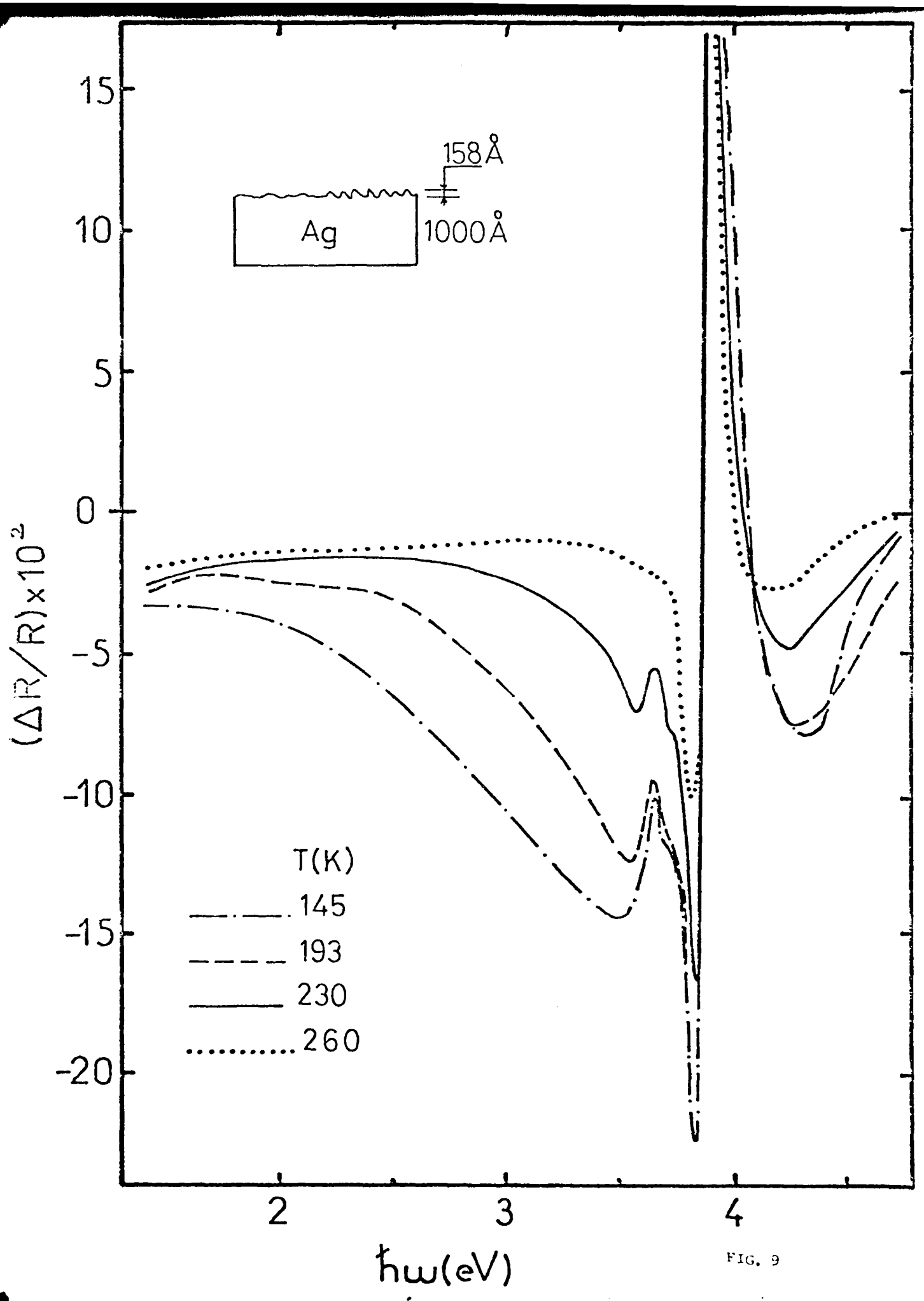
158Å
Ag
1000Å
T(K)
145
193
230
260
$(\Delta R/R)\times 10^{2}$
$\hbar\omega$(eV)

FIG. 9

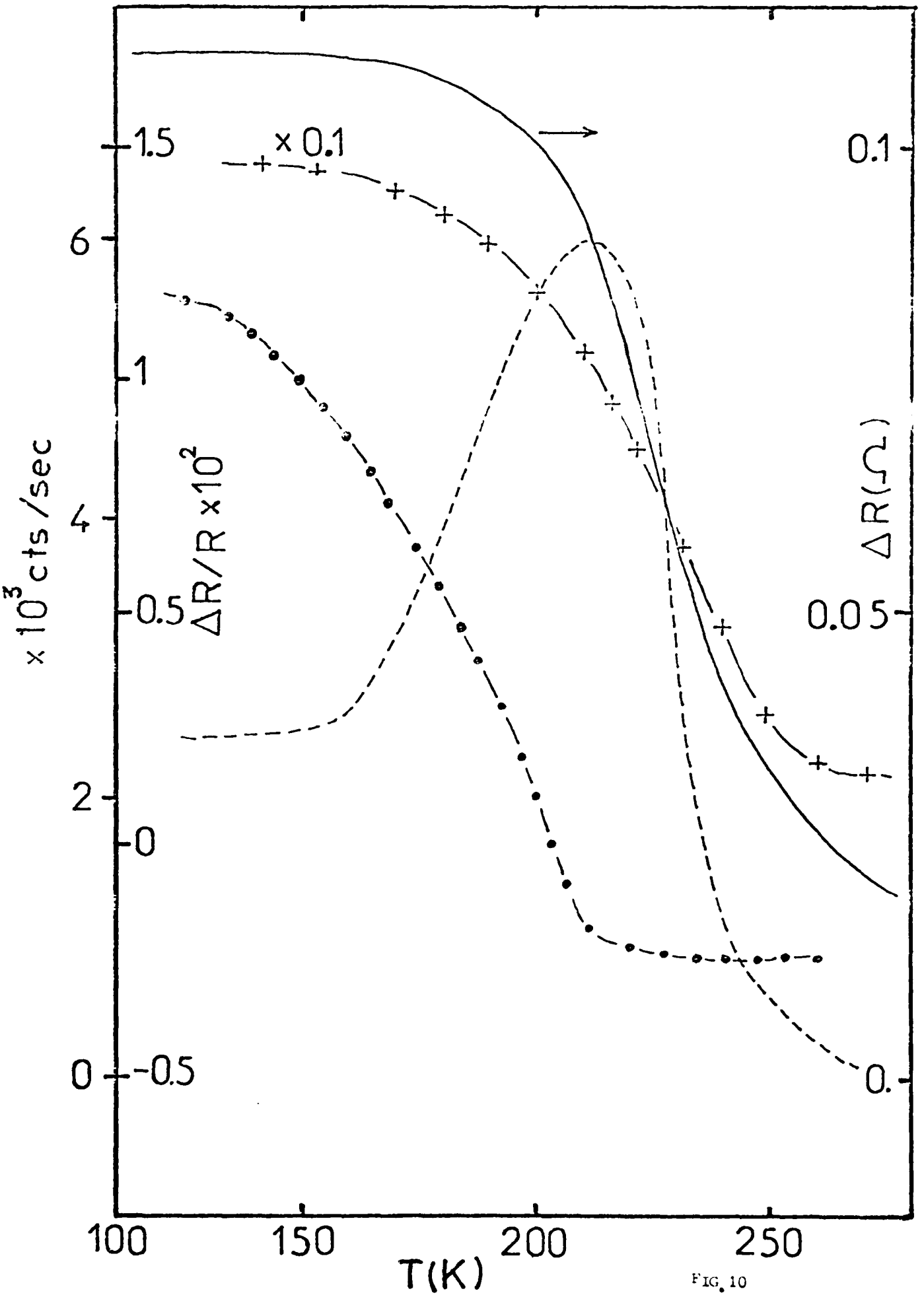
x 0.1
1.5
6
1
4
0.5
2
0
0
-0.5
0.1
0.05
0.
x 10^3 cts/sec
ΔR/R x10^2
ΔR(Ω)
100
150
200
250
T(K)

FIG. 10

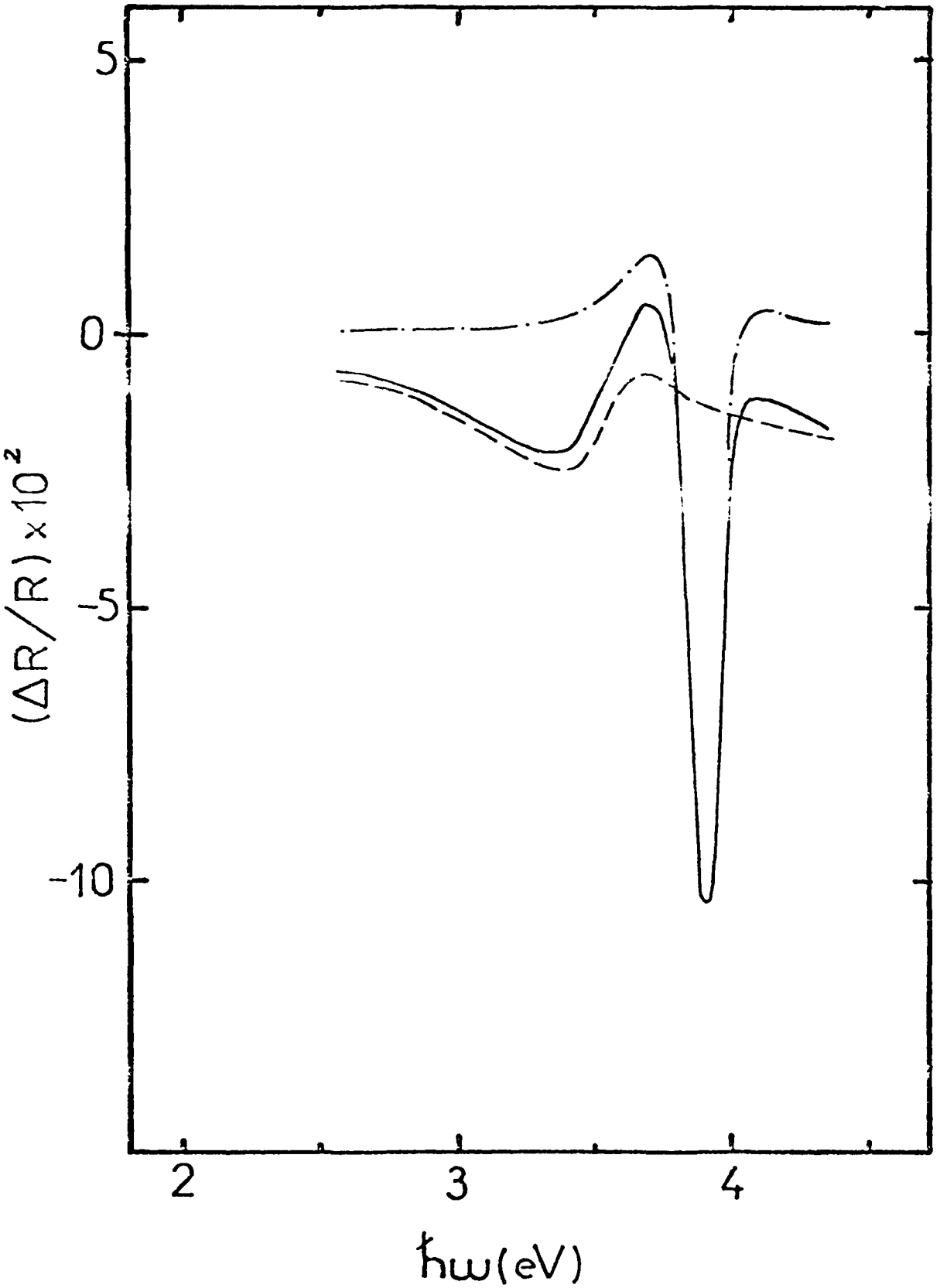

FIG. 11

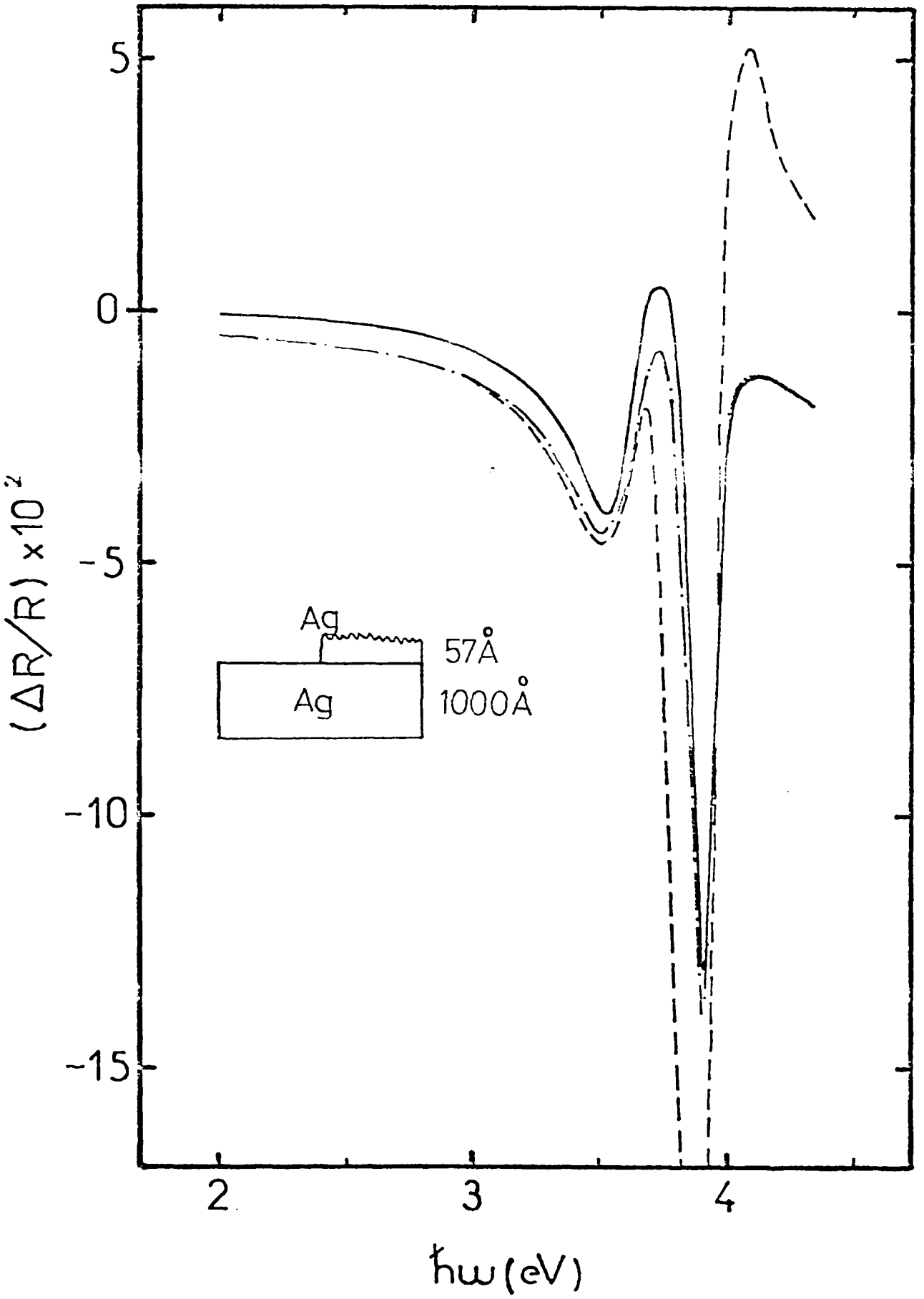

FIG. 12

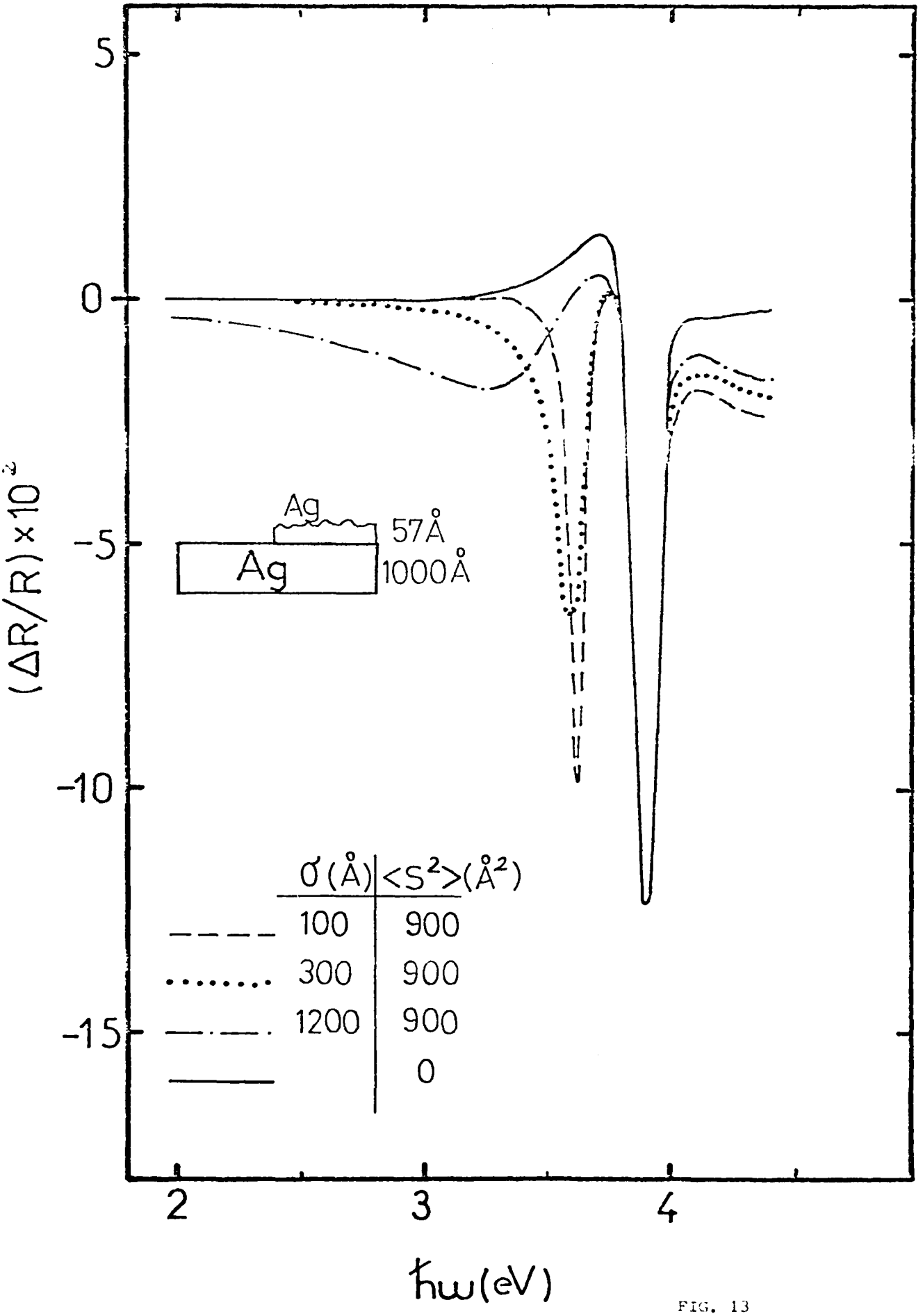
5
0
-5
-10
-15
2
3
4
$(\Delta R/R) \times 10^2$
$\hbar\omega$(eV)
Ag
57Å
Ag
1000Å
σ(Å) | <S²>(Å²)
100 | 900
300 | 900
1200 | 900
0

FIG. 13

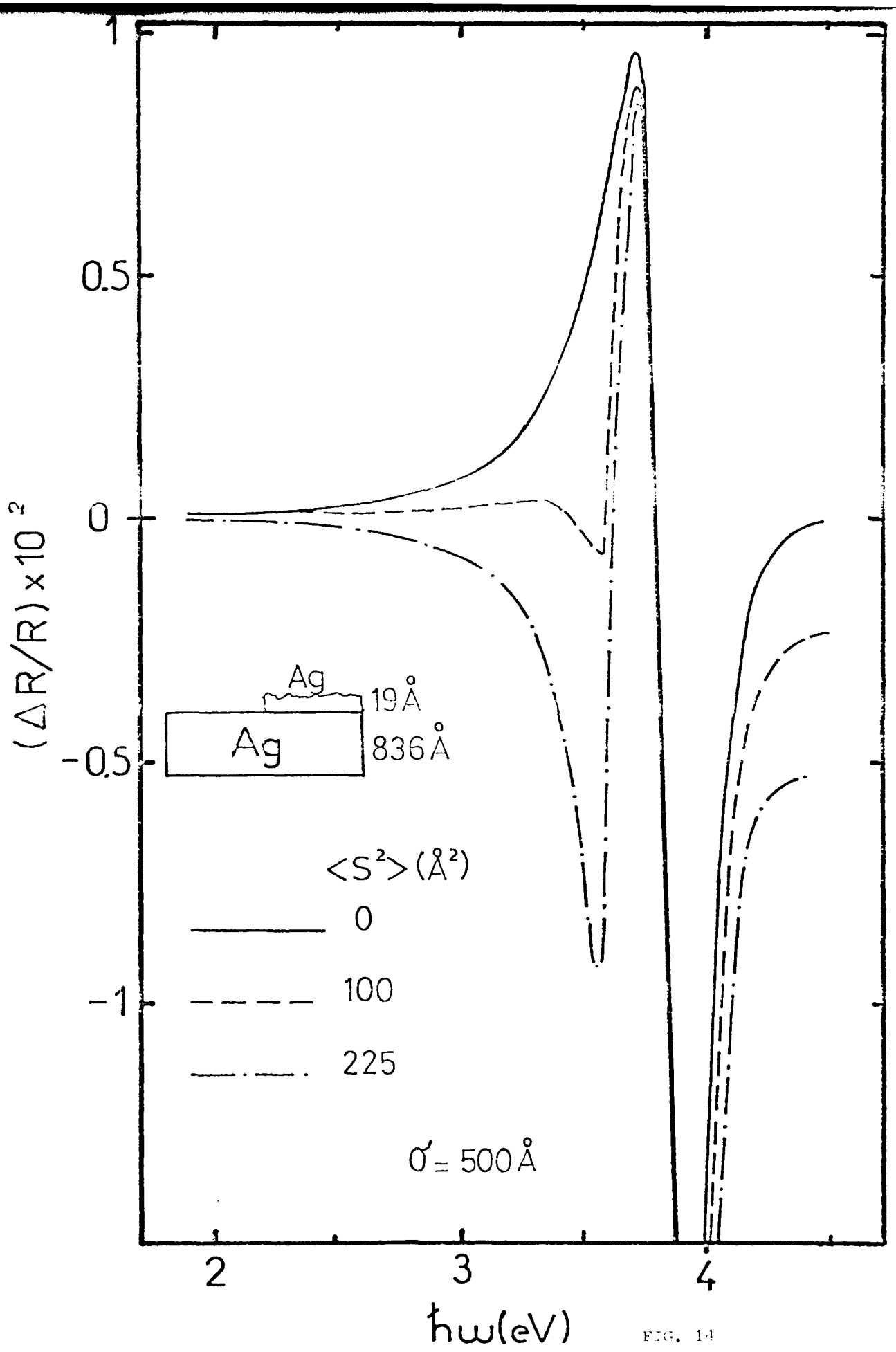
1
0.5
0
-0.5
-1
$(\Delta R/R) \times 10^{-2}$
Ag
19 Å
Ag
836 Å
$\langle S^2 \rangle$ (Å^2)
0
100
225
σ = 500 Å
2
3
4
$\hbar\omega$(eV)

FIG. 14

(a)

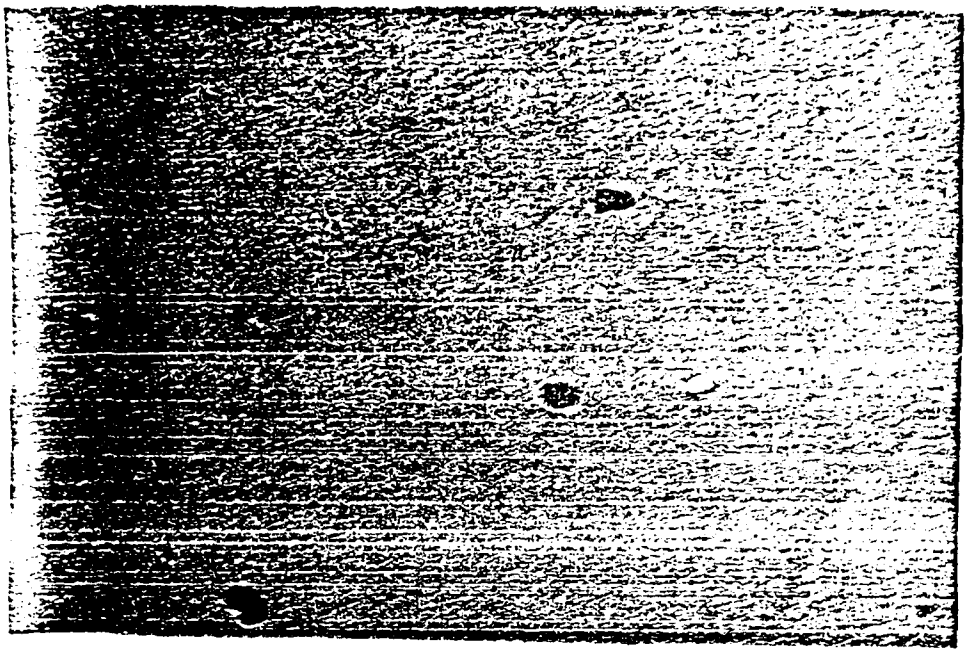

1000 Å

(b)

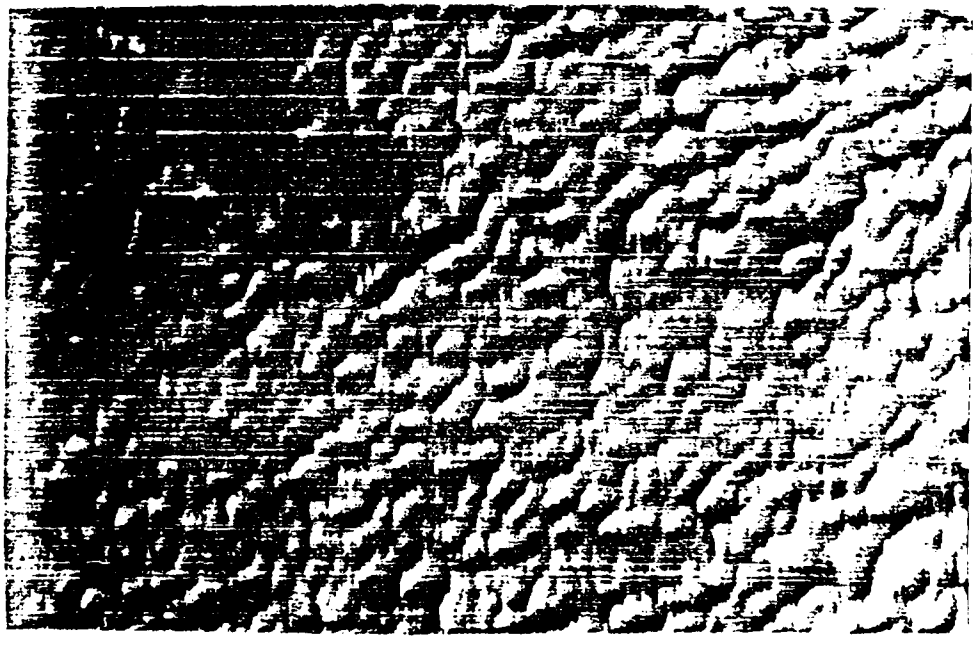

1000 Å

FIG. 15

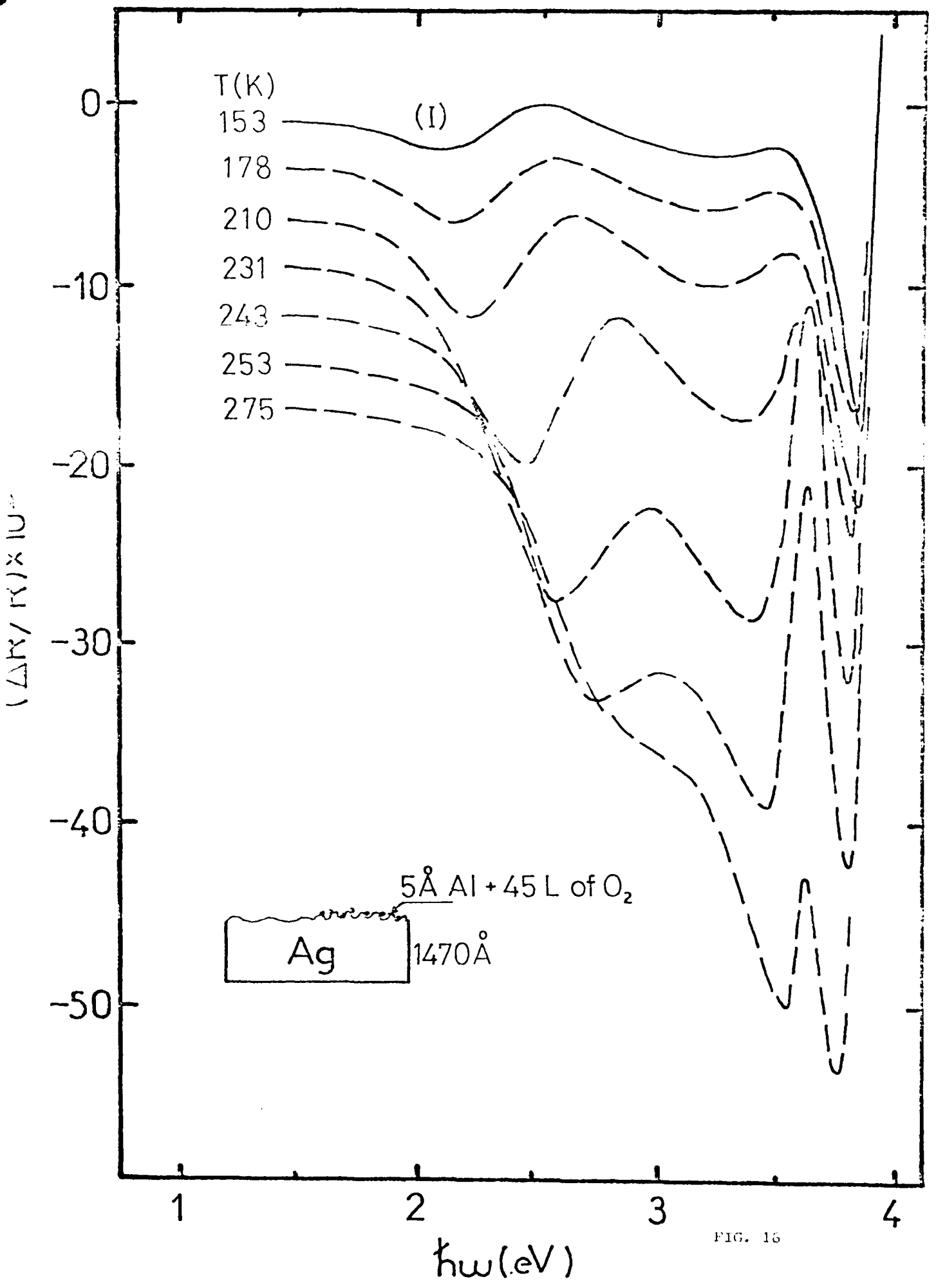
T(K)
153
178
210
231
243
253
275
(I)
0
-10
-20
-30
-40
-50
(ΔR/R)×10
5Å Al + 45 L of O2
Ag
1470Å
1
2
3
4
ħω(eV)

FIG. 16

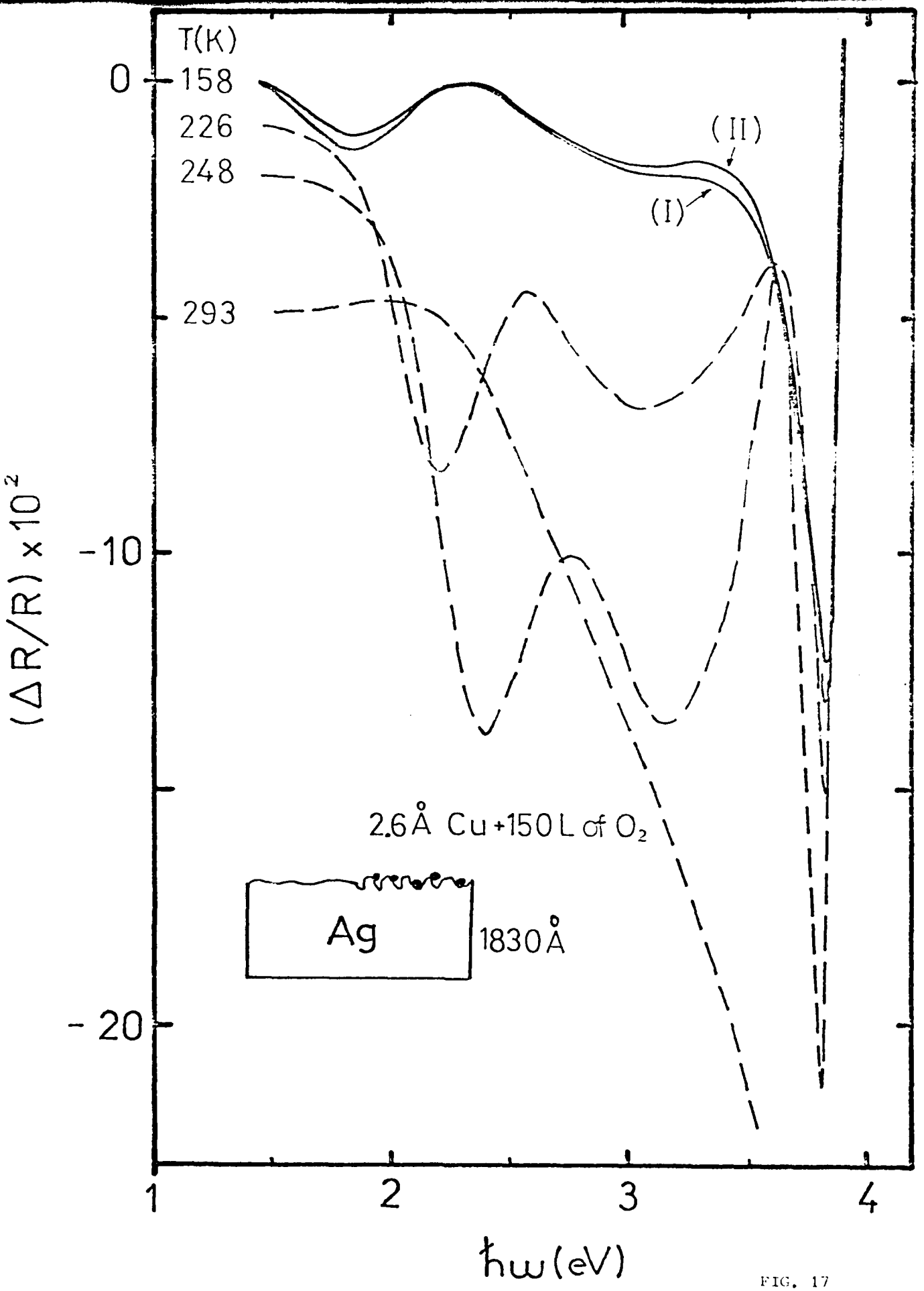
T(K)
158
226
248
293
(II)
(I)
0
-10
-20
$(\Delta R/R) \times 10^{-2}$
2.6Å Cu+150 L of O_2
Ag
1830Å
1
2
3
4
$\hbar\omega$(eV)

FIG. 17

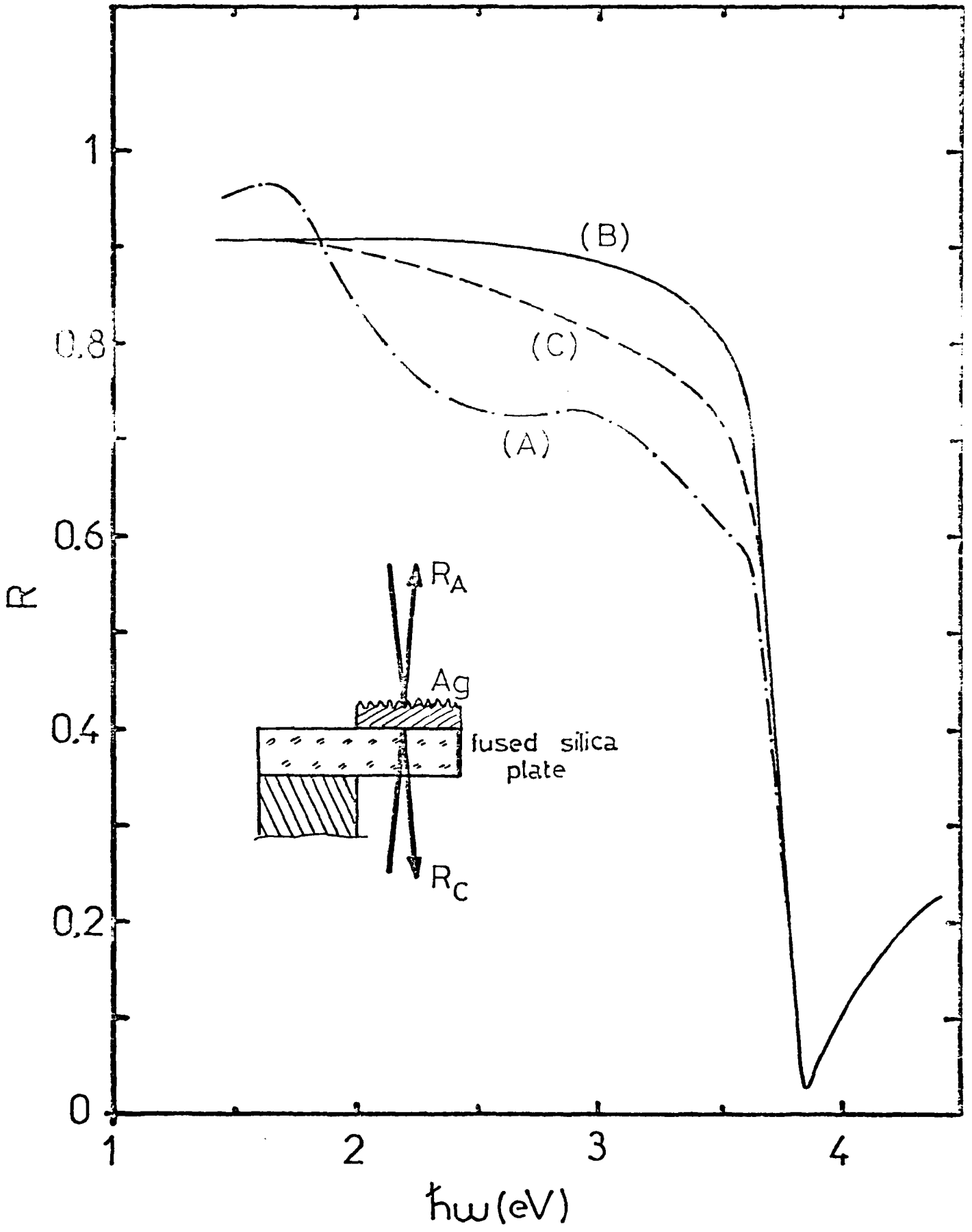

FIG. 13